International Journal of Coal Science & Technology (2025) 12:13
https://doi.org/10.1007/s40789-024-00731-8

REVIEW

Cerchar abrasivity test and its applications in rock engineering: A review

Guangzhe Zhang[1,2] · Kurosch Thuro[2] · Zhengyang Song[3,4] · Wengang Dang[5] · Qingsheng Bai[6,7]

Received: 28 December 2023 / Revised: 16 March 2024 / Accepted: 13 August 2024

Abstract

Abrasiveness as an intrinsic property of rocks defines the extent of wear or loss when interacting with other materials. In engineering sectors like hard rock mining and tunnelling, comprehending rock abrasiveness holds paramount importance due to its direct effect on tool wear during excavation. Among the diverse methods for assessing rock abrasiveness, the Cerchar abrasivity test emerges as the most widely used approach. Over time, the Cerchar test has garnered substantial attention from scholars, who have delved into the factors influencing test results due to testing conditions and examined the connection between the physical-mechanical parameters of rocks and their abrasiveness. Recent advancements in testing instrument have expanded our ability to measure additional parameters during rock cutting or drilling, yielding fresh insights for abrasiveness assessment, tool wear prediction, tool performance evaluation and rock excavatability estimation. The Cerchar abrasivity test, coupled with recent developments in testing instrument and parameter measurement, holds promising potential for enhancing our comprehension of rock abrasiveness and its practical implications. This review systematically traces the evolution of the test. It commences with an overview of the test origin and progression, emphasizing its pivotal role in assessing rock abrasiveness. Furthermore, it consolidates and categorizes the research contributions from various scholars regarding the test. This includes enhancements and refinements of the testing apparatus, as well as investigations into various testing orientations and their effects on different types of rocks. Moreover, this review illuminates the broader applications and interdisciplinary possibilities of this test, not only in material science but also in tribology. It underscores how the insights gleaned from the Cerchar test can be extrapolated to diverse areas of research beyond the scope of rock engineering.

✉ Guangzhe Zhang
guangzhe_zhang@hotmail.com

1 Institute of Foundation Engineering, China Academy of Building Research, Beijing 100013, People's Republic of China

2 Chair of Engineering Geology, TU Munich, 80333 Munich, Germany

3 School of Civil and Resource Engineering, University of Science and Technology Beijing, Beijing 100083, People's Republic of China

4 Chair of Engineering Geology, RWTH Aachen University, 52064 Aachen, Germany

5 School of Civil Engineering, Sun Yat-Sen University, Zhuhai 519082, People's Republic of China

6 Institute of Geosafety, School of Engineering and Technology, China University of Geosciences Beijing, Beijing 100083, People's Republic of China

7 Chair of Rock Mechanics and Rock Engineering, TU Bergakademie Freiberg, 09599 Freiberg, Germany

Article Highlights

- A comprehensive review on the Cerchar abrasivity test was performed
- Testing condition-based factors affecting the Cerchar values were studied
- Correlations of abrasive with physical-mechanical-mineralogical-petrographical properties of rocks were investigated
- Applications of Cerchar test in material science, tribology and rock engineering were discussed

Published online: 14 February 2025

Keywords Cerchar abrasivity · Cutting/drilling efficiency · Rock excavatability · Scratch test · Tool wear/performance

List of symbols

a	Radial wear of disc cutter (mm)
A_i	Percentage of individual constituent minerals within the rock (%)
AE	Acoustic emission
AV	Abrasion value on tungsten carbide (mg)
AMC	Abrasive mineral content (–)
AVS	Abrasion value on cutter steel (mg)
ANNA	Artificial neutral network analysis
ASTM	American society of testing materials
ANOVA	Analysis of variance
Al_2O_3	Aluminum
$B_1/B_2/B_3/B_4$	Brittleness index (–)
BA	Böhme abrasion (cm^3/50 cm^2)
BL	Bit working life (m/bit)
BHN	Brinell hardness number (3000 kgf)
BTS	Brazilian tensile strength (MPa)
BWI	Bit wear index
c_v	Wear coefficient (mm/km)
C	Carbon
Cr	Chromium
C_{Fsp}	Feldspar content (%)
C_{Qtz}	Quartz content (%)
CD	Cement degree (%)
CL	Cutter life (m^3/cutter)
CAI	Cerchar abrasivity index (0.1 mm)
CAI_x	Cerchar abrasivity index using HRC x (0.1 mm)
CAI_{40}	Cerchar abrasivity index using HRC 40 (0.1 mm)
CAI_{55}	Cerchar abrasivity index using HRC 55 (0.1 mm)
CAR	Cerchar abrasion ratio (mm^3/mm^3)
CC(R)	Cutter consumption (rate) (cutters/m^3)
CEI	Cerchar excavatability index (N/mm)
CLI	Cutter life index (mm/mg)
CSE	Cerchar specific energy (mJ/mm^3)
CSM	Colorado school of mines
Cerchar	Centre d'Etudes et Recherches des Charbonnages de France
d	Tip wear flat (mm)
d_{Fsp}	Feldspar grain size (mm)
d_{Qtz}	Quartz grain size (mm)
D	Diameter of disc cutter (mm or feet)/Tunnel diameter (m)
DEM	Discrete element method
DoP	Penetration depth/Depth of scratch/cut (mm or μm)
DRI	Drilling rate index (–)
DSS	Direct shear strength (MPa)
E	Young's modulus (GPa)
E_f	Average cutter life (m^3/mm)
EQC	Equivalent quartz content (%)
F_N	Applied load (N)
F_T	Thrust force (N)
$F_Ø$	Ferret's diameter (mm)
Fsp	Feldspar
F-index	Schimazek wear index (N/mm)
GEP	Gene expression programming
H_K	Knoop hardness number (N/mm^2)
$H_{M(i)}$	Mohs hardness number (of individual minerals) (–)
$H_{V(i)}$	Vickers hardness number (of individual minerals) (kgf/mm^2)
$H_{R(i)}$	Rosiwal hardness number (of individual minerals) (–)
HRC	C scale of Rockwell hardness number (–)
Is_{50}	Point load index (MPa)
ISRM	International society for rock mechanics and rock engineering
K_{IC}	Fracture toughness Mode-I
L	Cutter life/Rolling length (m)/Excavated tunnel length (m)
L_s	Scratching distance (mm)
LF	Cutter life (10^6 feet)
LAC	LCPC abrasivity coefficient (g/t)
LCPC	Laboratoire Central des Ponts et Chausées
M	Rock moisture (%)/Total wear extent of all disc cutters (mm)
Mn	Manganese
Mo	Molybdenum
MSF	Mean scratching force (N)
MCAI	Modified Cerchar abrasivity index (0.1 mm/N)
MDWR	Mini disc wear rate (g/m^3)
n	Porosity (%)/Numbers of constituent minerals within the rock (–)
Ni	Nickel
N_{Peak}	Number of peaks (–)
NTNU	Norwegian university of science and technology
Opa	Opaque mineral
p	Confining pressure (MPa)
P	Perimeter (mm) / Phosphorus
PFC	Particle flow code
Plg	Plagioclase
PPI	Punch penetration index (MPa)
Qtz	Quartz
R	Roughness
RAI	Rock abrasivity index (–)
RME	Rock mass excavatability index (–)
ROP	Rate of penetration (mm/s)

RIAT	Rolling indentation abrasivity test
$RIAT_a$	RIAT abrasivity index (mg)
R^2	Coefficient of determination
S	Sulfur
Si	Silicon
S_{20}	Brittleness value (%)
S_r	Rolling distance of disc cutter (km)
SE	Scratching energy (Nmm or mJ)
SF	Scratching force (N)
SJ	Sievers' J-value (mm/10)
SE_i	Scratch energy index (kJ/cm^3)
SAT	Soil abrasion test
SEM	Scanning electron microscope
SHH	Schmidt hammer hardness (N/mm^2)
SSH	Shore scleroscope hardness (N/mm^2)
SiO_2	Silica
T	Width of cutter ring (mm)
TC	Tool consumption (tools/m^3) or (tools/t)
TL	Diameter reduction of disc cutter (mm)
TBM	Tunnel boring machine
UCS	Uniaxial compressive strength (MPa)
UTS	Ultimate tensile strength (MPa)
v_P	P-wave velocity (km/s or m/s)
V	Vanadium
V_m	Material removal volume (mm^3)
V_s	Tip wear volume (mm^3)
VHNR	Vickers hardness number of rock (%)
w	Wear flat of disc cutter (m)
W	Waveness / Tungsten
W_f	Specific weight loss (mg/m)
Wt	Weight percentage (%)
WWA	Wide wheel abrasion (mm)
θ	Wedge-shaped edge angle of disc cutter (°)
$\sigma_{1/2/3}$	Confinement on the Hoek's cell (MPa)
σ_c	Uniaxial compressive strength (MPa)
σ_m	Mean stress (MPa)
σ_{PLT}	Point load index (MPa)

1 Introduction

Abrasiveness of rocks is defined as wear or loss of material that rocks produce on another material (Atkinson 1993), especially on mechanical tools like tunnel boring machine (TBM) discs, roadheader picks and drill bits, as illustrated in Fig. 1. The significance of rock abrasiveness cannot be ignored, as it directly affects tool wear, cutting or drilling efficiency, excavation effectivity, energy consumption, as well as project time and costs. Seen from Fig. 2, assessing rock abrasiveness relies on determining tool wear resistance in direct contact with rocks involving a range of measurements. Such measurements comprise different scales ranging from real-scaled tests with actual excavators, through model tests with simplified tools, to mechanical and mineralogical analyses of rocks and constituent minerals. Table 1 summarizes the most frequently used model testing methods for assessing rock abrasiveness, and a comprehensive review of these methods can refer to Cassapi (1987), Okubo et al. (2011), Janc et al. (2020), Hamzaban et al. (2023) and Mucha (2023). Among the model tests, the Cerchar abrasivity test is the most widely used method for assessing rock abrasiveness. Its popularity arises from its simple design and ease of use. This test can be conducted directly on-site due to straightforward setup and user-friendly measurements. This practicality and efficiency make it an invaluable method for assessing rock abrasiveness during fieldwork.

Since the inception of the Cerchar test, numerous scholars have conducted studies to explore the influences of various factors. These factors fall into two: (1) Testing condition-based factors: These factors pertain to the testing apparatus, rock surface roughness, stylus hardness and metallurgy, testing distance and velocity, as well as approach used to measure the tip wear; (2) Geological-geotechnical factors: These factors relate to the constituent minerals of rocks, including their composition and content and grain attributes (i.e., size, shape and hardness), as well as the intrinsic properties of rocks, such as strength, brittleness and toughness. Understanding the sensitivity of Cerchar results to the testing instrument, procedure and measurement approach is crucial for ensuring the reliability and repeatability of this test. Investigating the rock intrinsic properties is essential to ascertain how these properties affect the abrasive potential of rocks, and vice versa.

The primary objective of this review is to present a comprehensive account of the state of the art in research on the Cerchar abrasivity test, and herein lays its originality. We use the literatures to provide a global perspective of published articles and highlight potential areas for future research based on this test. The remainder of this paper is organized as follows: Section 2 presents an overview of the Cerchar testing method, which covers diverse aspects including test development and methodology, modifications of testing devices and their practical engineering applications, offering insights into research related to this method for assessing rock abrasiveness. Section 3 contains a detailed discussion of testing condition-based factors influencing the Cerchar results, especially surface condition, stylus hardness, testing distance and velocity and tip wear measurement. Section 4 provides a comprehensive analysis of rock intrinsic properties to see how abrasiveness develops in different rock materials with respect to their mineralogical and mechanical properties. In Sect. 5, we delve into the potential applications of the Cerchar test in different research areas. The opportunities and advantages of using this test to analyze material property of various tool steels in material science, to verify abrasive wear phenomenon in tribology, as well

Fig. 1 Wear of typical mechanical tools (e.g., TBM discs, roadheader picks and drill bits) during hard rock excavations. (Thuro 1996; Thuro 2002; Ellecosta et al. 2018; Janc et al. 2020; Zhang et al. 2022b; Bołoz and Biały 2023, modified)

as to estimate rock-tool interaction and tool performance in rock engineering are noted.

2 Cerchar abrasivity test

2.1 Testing approach

The Cerchar abrasivity test, originally developed by the Centre d'Etudes et Recherches des Charbonnages de France (Cerchar) for the French coal mining industry (Valantin 1973), has been extensively documented and standardized. The detailed testing methodology is outlined by Cerchar (1986), the French standard of NF P94-430-1 (2000), the ASTM norm (ASTM D7625-10 2010) and the ISRM recommendation (Alber et al. 2014).

2.2 Testing apparatus

Two generations of testing apparatuses have been designed since the test inception: (1) The original Cerchar apparatus fabricated in the Cerchar center (Cerchar 1986); (2) The West apparatus designed by West (1986b), as illustrated in Fig. 3. These two apparatuses employ distinct testing principles. In the Cerchar apparatus, the stylus slides on a fixed rock sample for 1 s, while in West apparatus, the rock

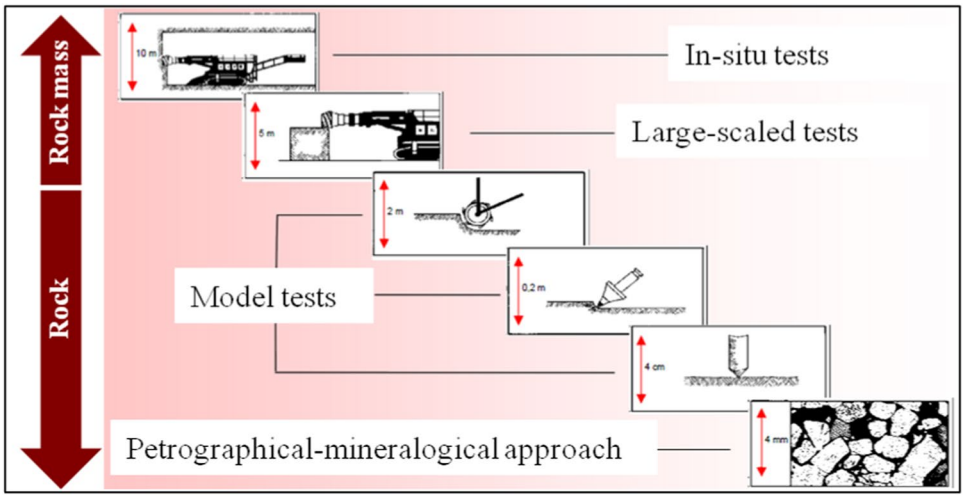

Fig. 2 Determination of rock abrasiveness at different scales (Plinninger 2015, modified)

Table 1 Model testing methods for abrasiveness determination of rock materials

Testing methods	References	Testing procedures	Applied tools	Rock materials	Indexes
NTNU SAT test	Selmer-Olsen and Lien (1960)	Weight loss of steel piece	Steel piece	Rock powder (< 1 mm)	AV/AVS (mg)
Cerchar test	Cerchar (1986)	Truncation of stylus tip	Steel stylus	Intact rock sample	CAI (0.1 mm)
LCPC test	NF P18-579 (1990)	Weight loss of metal impeller to rock aggregates	Metal impeller	Rock aggregates (4.0–6.3 mm)	LAC (g/t)
RIAT test	Macias et al. (2015)	Weight loss of miniature cutter ring	Miniature disc cutter	Intact rock sample	$RIAT_a$ (mg)
Böhme test	EN 14157 (2017)	Volume loss of rock sample	Abrasive grain (e.g. corundum)	Cubic rock sample	BA (cm^3/50 cm^2)
Wide wheel test	EN 14157 (2017)	Wide of groove on rock surface	Abrasion wheel	Cubic rock sample	WWA (mm)

sample moves beneath the stationary stylus for duration of 10 s. Subsequent apparatuses are the modifications or derivations of these two foundational designs.

2.3 Testing procedure

The testing procedure involves securely clamping a suitable rock sample using a rigid vice. This setup enables the stylus to perform the scratching operation on the rock surface. Prior to scratching, the stylus is carefully lowered onto the sample surface to avoid any damage to the stylus tip. The steel stylus undergoes heat treatment to achieve a Rockwell hardness number of HRC 54–56 or HRC 40–42 (depending on the rock strength). Table 2 provides the material properties of applied tool steels by Cerchar (1986) and West (1989). The stylus with a conical tip angle of 90° is positioned orthogonal to the sample surface and then loaded with a constant normal load of approximately 70 N (equivalent to a 7 kg weight). The stylus moves a total distance of 10 mm at a velocity of 1 mm/s or 10 mm/s (depending on the applied apparatus). After each scratch test, the wear flat on the stylus tip is measured in millimeter under a digital binocular, as shown in Fig. 4, by which the correct angle of 90° on the tip is reproduced. The Cerchar abrasivity index (CAI) is then calculated by multiplying the wear flat with a factor of 10. Five single scratches with new or refurbished styli are repeated to obtain the final CAI value for a rock sample. The classification of rock abrasiveness according to CAI is provided in Table 3, and this classification is derived from CAI measurements on rough rock surfaces. Figure 5 summarizes the CAI values and variations for different rock materials.

2.4 Newly designed Cerchar testing device

Recently, new Cerchar testing devices have been developed to enhance measurement accuracy and to provide valuable insights for evaluating cutting or drilling efficiency in rock engineering. Figures 6a, 7a, 8a and 9a depict the modified Cerchar testing devices currently in use around the world.

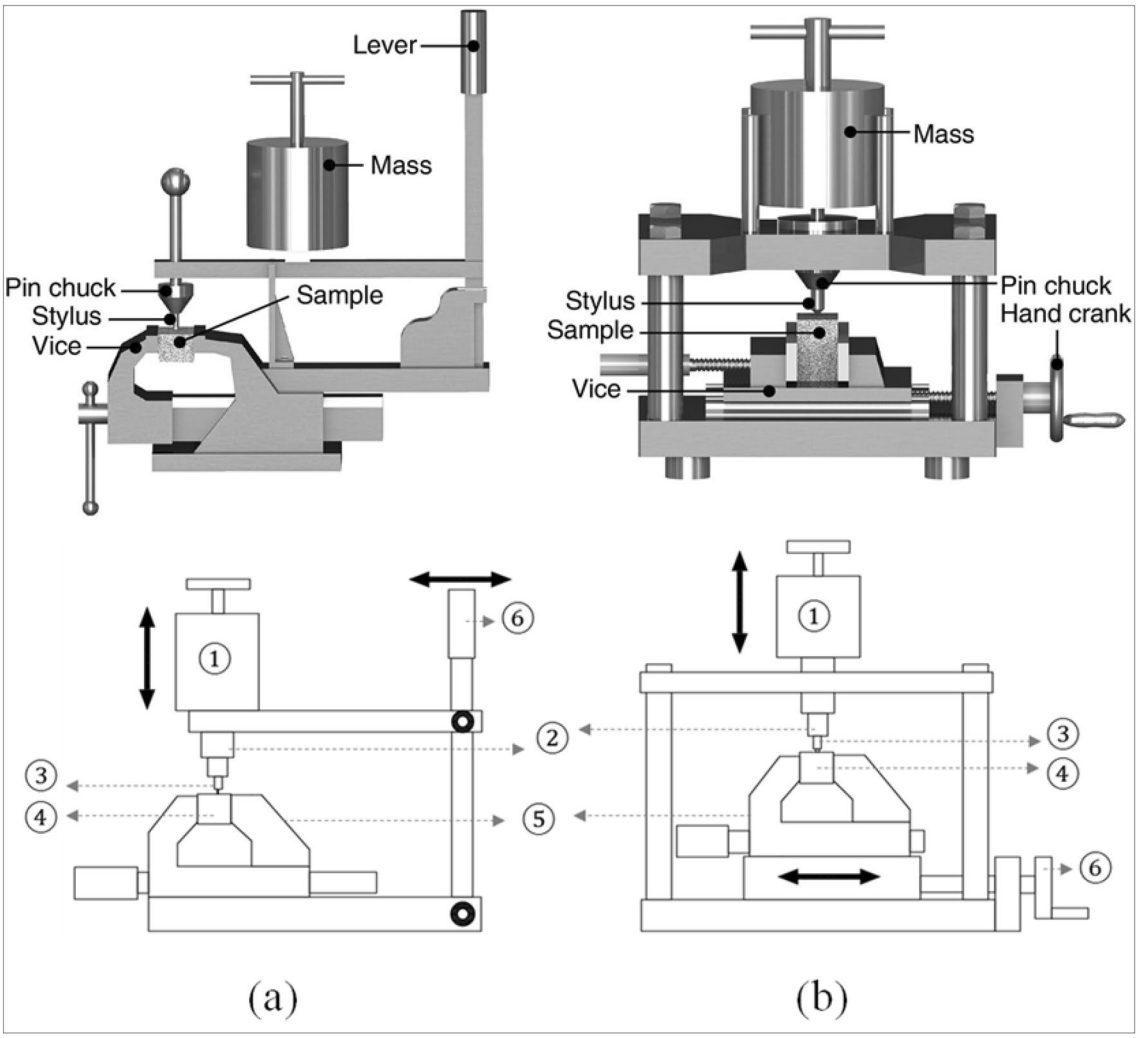

Fig. 3 View on the **a** Cerchar apparatus and **b** West apparatus (① Normal load; ② Stylus guide; ③ Steel stylus; ④ Rock sample; ⑤ Vice; ⑥ Hand lever/crank) (Cerchar 1986; West 1989; Alber et al. 2014; Gao et al. 2024, modified)

Table 2 Material properties of applied tool steels (Stanford and Hagan 2009)

References	Ultimate tensile strength (UTS) (MPa)	C scale of Rockwell hardness number (HRC) (–)	Vickers hardness number (H_V) (kgf/mm^2)	Brinell hardness number (BHN) (3000 kgf)	Shore scleroscope hardness (SSH) (N/mm^2)
Cerchar (1986)	2000	54–56	633	595	76
West (1989)	1255	40	392	371	54

In essence, all these devices are designed to enable performing the Cerchar test by a servo-controlled system and with various sensors. These devices incorporate a couple of sensors, which are fixed to the Cerchar or West apparatus to monitor the displacements (horizontal and/or vertical) and forces (normal and/or scratching) during scratching. A data acquisition system is adopted to collect and store data from different sensors. A computer program governs the device, enabling users to specify input parameters and proceeds to record force-displacement data automatically. For instance, Figs. 9b–i illustrates the distinctive variations in scratching force curves among different types of rocks. It is evident that, for fine-grained rocks (e.g., slate, dolomite and limestone), relatively minor fluctuations in scratching forces are observed. Conversely, for medium-grained heterogeneous rocks (e.g., granite and diorite), significant fluctuations in scratching forces usually arise. Particular noteworthy is the substantial fluctuation in scratching force observed for gneiss. This phenomenon can be attributed to the stylus transitioning from soft and non-abrasive mica-rich layers to the hard and abrasive quartz-rich layers.

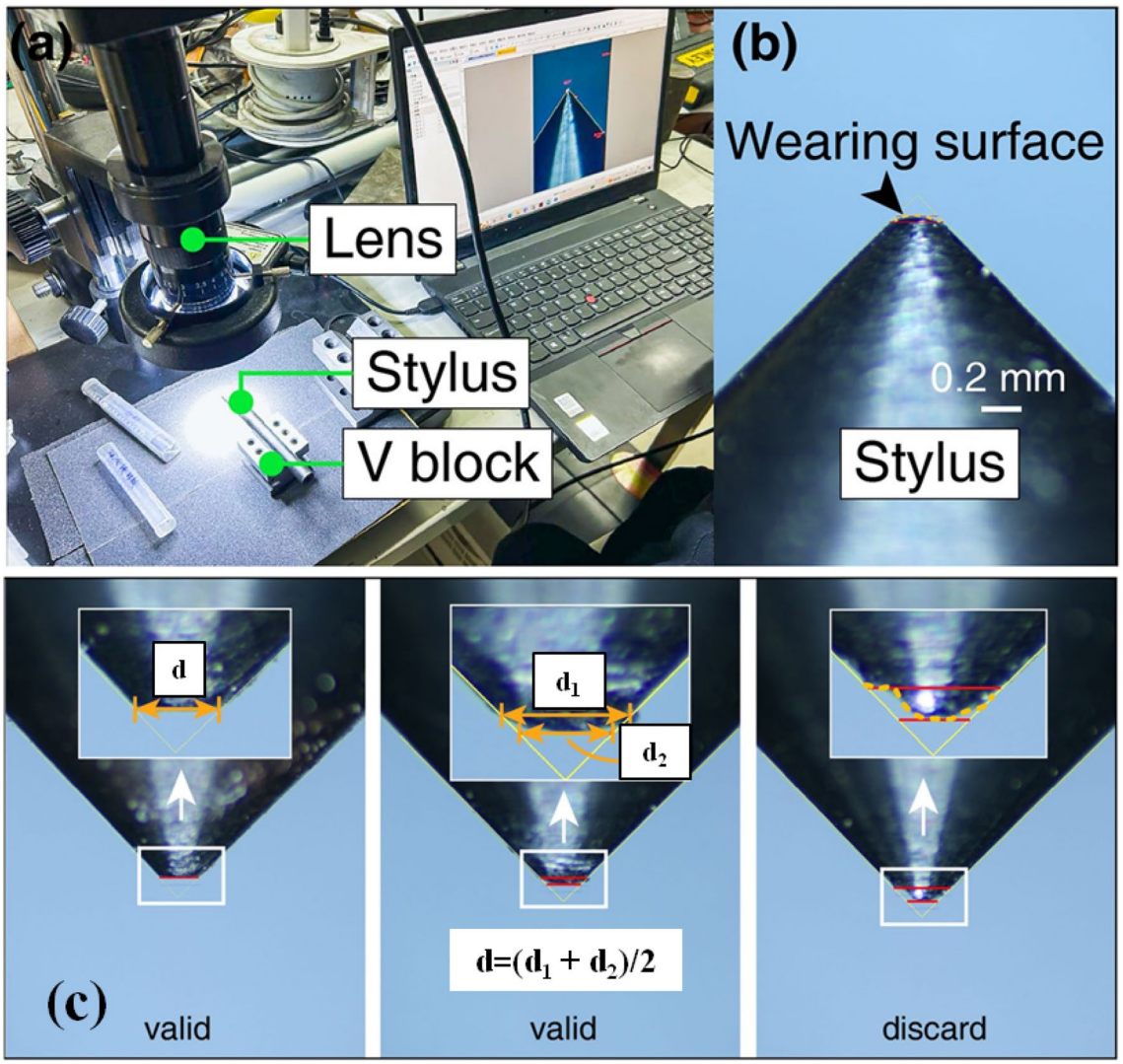

Fig. 4 Measurement of wear flat on the stylus tip using digital binocular (Gao et al. 2024)

After each scratch test, a digital microscope is used to ascertain both the depth of the scratch inflicted on the sample surface and the material volume removed from the rock, as illustrated in Figs. 10a–c. For instance, Fig. 10d provides a concise overview of the penetration depth of the stylus in different types of rocks. Consequently, the modified Cerchar testing device facilitates the measurements and records of numerous essential parameters pertinent to rock cutting and drilling in rock engineering. Figure 11 presents a flowchart delineating the steps involved in determining the rock cutting- or drilling-related parameters, Figure 12 and Table 4 succinctly encapsulate the definitions, determination methods and practical applications of these parameters. Three most important parameters and their applications are described as follows: (1) The Cerchar specific energy (CSE) calculated as the ratio of scratching energy to material removal volume can be used to assess the rock abrasiveness, to estimate the rock-stylus interaction, as well as to evaluate the efficiency of rock scratching, which can further be referred to as an indicator for rock cutting or drilling efficiency; (2) The Cerchar abrasion ratio (CAR) relates the two volumetric parameters — the material volume removed from the rock surface and the wear volume abraded on the stylus tip, and can be used to estimate the interaction between the rock and mechanical tool during cutting and to evaluate the cutting effectivity; (3) The Cerchar excavatability index (CEI), which is defined as the ratio of scratching force to the depth of scratch, can be used to estimate the rock excavatability (i.e., cuttability and drillability), which reflects the facility of rocks to be excavated by mechanical tools.

Table 3 Classification of rock abrasiveness according to CAI

Cerchar specification (Cerchar 1986)		
CAI (0.1 mm) (HRC 54–56)		Classification
0.3–0.5		Not very abrasive
0.5–1.0		Slightly abrasive
1.0–2.0		Medium abrasive to abrasive
2.0–4.0		Very abrasive
4.0–6.0		Extremely abrasive
ASTM norm (ASTM D7625-10 2010)		
CAI (0.1 mm) (HRC 55)	CAI (0.1 mm) (HRC 40)	Classification
0.3–0.5	0.32–0.66	Very low abrasive
0.5–1.0	0.66–1.51	Low abrasive
1.0–2.0	1.51–3.22	Medium abrasive
2.0–4.0	3.22–6.62	High abrasive
4.0–6.0	6.62–10.03	Extremely abrasive
6.0–7.0	N.A	Quartzitic
ISRM recommendation (Alber et al. 2014)		
CAI (0.1 mm) (HRC 54–56)		Classification
0.1–0.4		Extremely low abrasive
0.5–0.9		Very low abrasive
1.0–1.9		Low abrasive
2.0–2.9		Medium abrasive
3.0–3.9		High abrasive
4.0–4.9		Very high abrasive
≥ 5.0		Extremely high abrasive

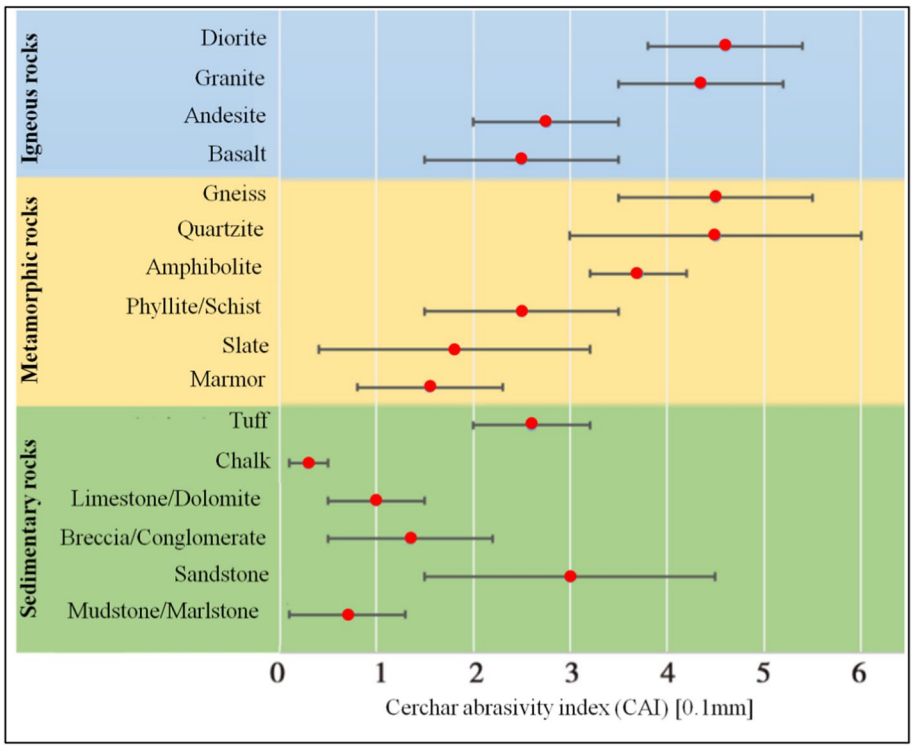

Fig. 5 CAI values and variations for various types of rocks (e.g., metamorphic, sedimentary, igneous) (Gong et al. 2021, modified)

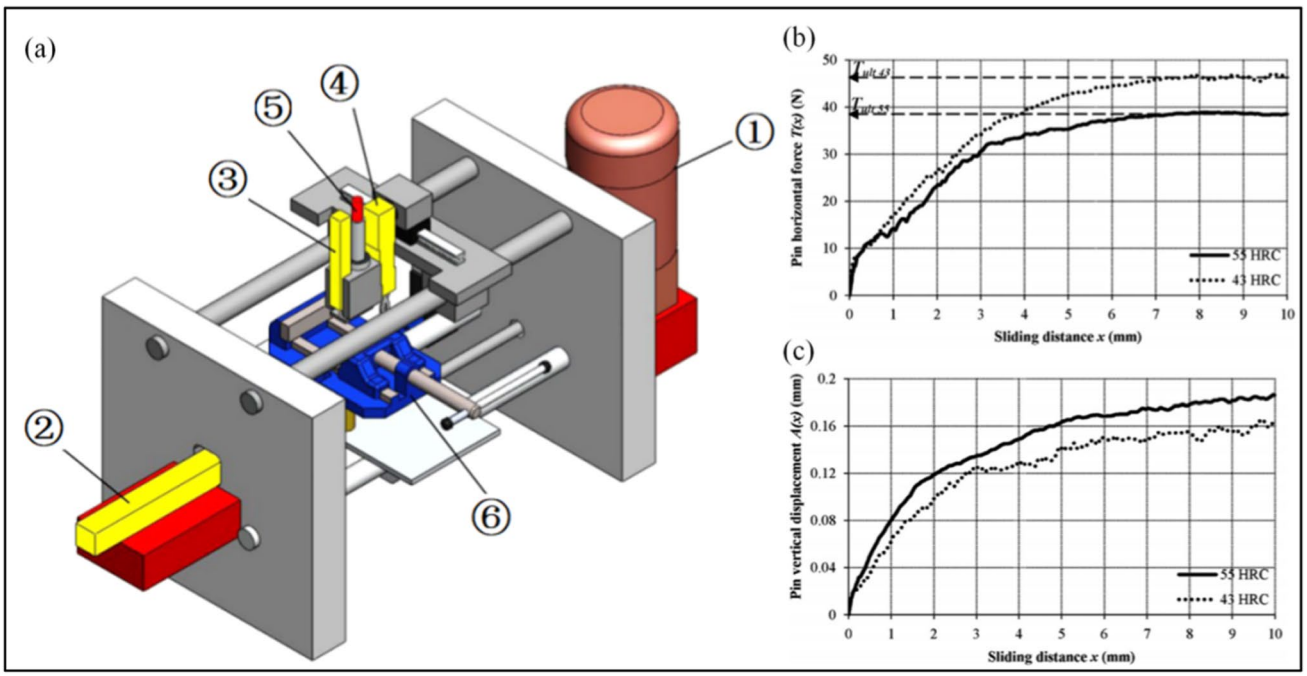

Fig. 6 **a** View on a modified Cerchar testing device (① Electric motor; ② Horizontal displacement sensor; ③ Vertical-displacement sensor; ④ Load cell; ⑤ Stylus; ⑥ Vice); Measurement of **b** Applied scratching force and **c** Penetration depth of the stylus within the rock under the application of two styli (HRC 55 vs. HRC 43) (Hamzaban et al. 2014)

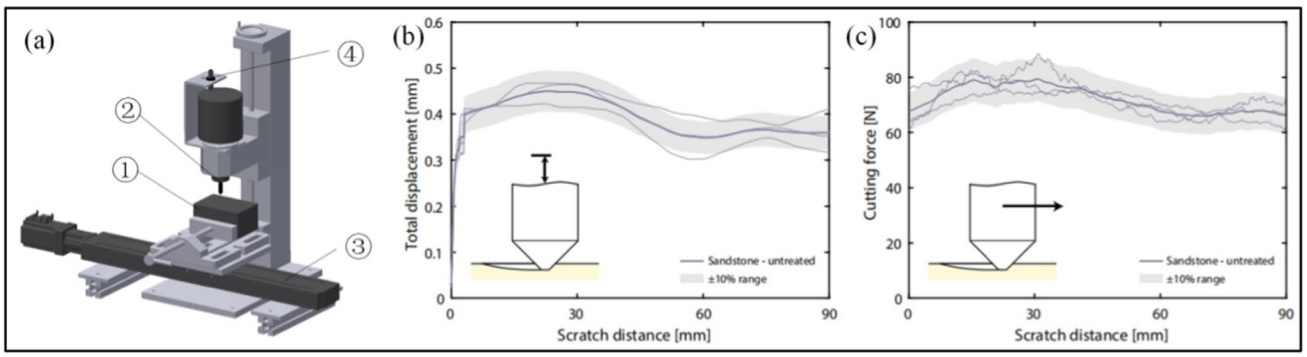

Fig. 7 **a** View on a modified Cerchar testing device (① Rock; ② Stylus; ③ Horizontal force and displacement sensor; ④ Vertical displacement sensor); Measurement of **b** Penetration depth of the stylus within the rock and **c** Applied scratching force for a sandstone sample (Rossi et al. 2018, 2020)

3 Influence of testing condition-based factors on CAI

3.1 Testing apparatus

Käsling et al. (2007) found that the CAI values measured with Cerchar apparatus are lower than those with West for heterogeneous rocks, and then concluded that the West apparatus is more stable. Sotoudeh et al. (2014) compared the CAI values determined from West apparatus and newly designed testing device (see Fig. 6a), and observed that, especially for abrasive rocks, the decrease in standard deviations of CAI values is more significant by using automatic testing device. They attributed this to the accurate control of testing distance and velocity.

3.2 Applied load

The applied load, approximately 70 N (equivalent to a 7 kg weight), results in varying contact stress due to tip wear. Jacobs and Hagen (2009) found that the Cerchar results

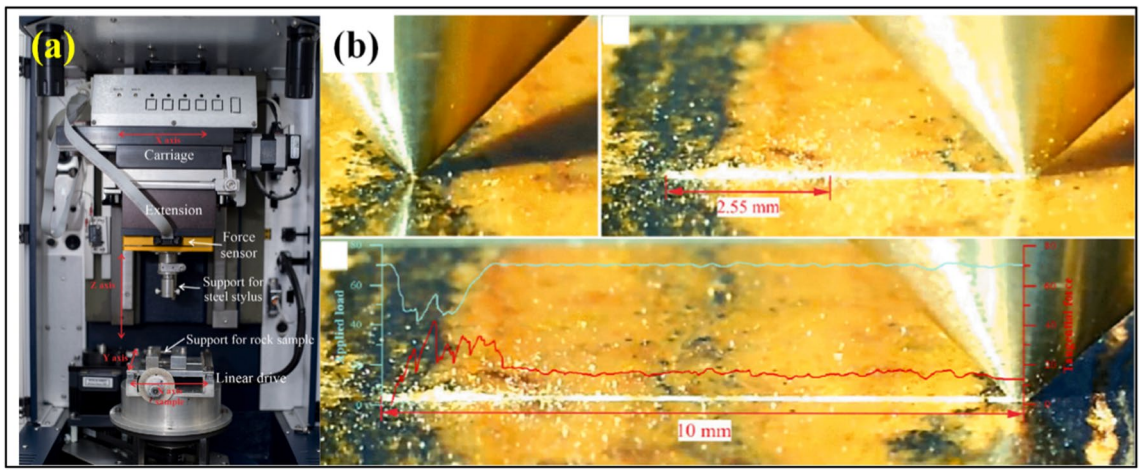

Fig. 8 **a** View on a modified Cerchar testing device used to measure **b** The normal load and scratching force, respectively (Münch et al. 2023)

remain insensitive to the applied load, when its value varies between 70 ± 2 N. Moreover, it is logical to expect an increase in tip wear, as the normal force increases (Ghasemi 2010; Rostami et al. 2014).

3.3 Surface condition

It is recommended using fresh-broken (rough) surface for testing, because such surface can closely mimic the actual rock cutting process, yielding conservative results for CAI (Cerchar 1986; ASTM D7625-10 2010; Alber et al. 2014). Fig. 13 shows that CAI values measured on fresh broken rock surfaces are generally higher than those on saw-cut rock surfaces. Plinninger et al. (2003) and ASTM D7625-10 (2010) suggested a linear correlation between rough and sawn surfaces, with rough surface showing approximately 0.48 higher CAI value. Rostami et al. (2005) noted that the difference of CAI values is more pronounced harder and more abrasive rocks like quartzite. They attributed this to with the high strength of rocks causing the stylus to gradually approach the sample surface. The so-called "skating-effect" can lead to an underestimation of CAI. Käsling and Thuro (2010) identified that CAI on sawn surface is roughly 88% of that on rough surface. Yarali and Duru (2016) similarly established a linear correlation, indicating an approximately 18% higher CAI value for rough surface. Er and Tuğrul (2016) delved into surface roughness, waveness and peak number, as illustrated in Fig. 14, revealing that increased surface roughness correlates with higher abrasiveness. However, Aydin (2019) stressed the importance of saw-cut surface, as it generally leads to lower measurement variability compared to rough surface.

3.4 Stylus hardness and metallurgy

The applied stylus should be heat-treated to HRC 54–56 (ASTM D7625-10 2010; Alber et al. 2014). However, variations in stylus metallurgies and hardnesses among different laboratories around the world emerged due to raw material problems. West (1989) used a stylus made from EN 24 steel and hardened to HRC 40. Al-Ameen and Waller (1994) highlighted that the hardness of EN 24 surpasses that of materials used for mining equipment, leading them to optional for a softer EN 3 stylus. In an effort to mitigate measurement inaccuracy stemming from stylus differences, Plinninger et al. (2003) suggested using the 115CrV4 tool steel, hardened to HRC 55 ± 1 as a reference. Michalakopoulos et al. (2006) established a linear correlation between two commonly used hardness levels: CAI at HRC 55 equates to roughly 60% of CAI at HRC 40. Stanford and Hagan (2009) also found a direct correlation between CAI and stylus hardness, especially for sandstone, where CAI decreases with increasing HRC. They emphasized that CAI remains insensitive to the metallurgical composition of stylus steel, as long as their hardness levels match. Moreover, Jacobs and Hagan (2009) gave a formula for calculating the CAI value of standard hardness of HRC 55 from other HRC numbers. Käsling (2009) obtained a linear correlation between two commonly used tool steels, CrV-steel vs. CrNiMo-steel. Table 5 provides the chemical compositions of several applied tool steels those have been used for the Cerchar testing.

3.5 Testing distance and velocity

In term of testing distance, Al-Ameen and Waller (1994) found that a substantial portion of tip wear, approximately

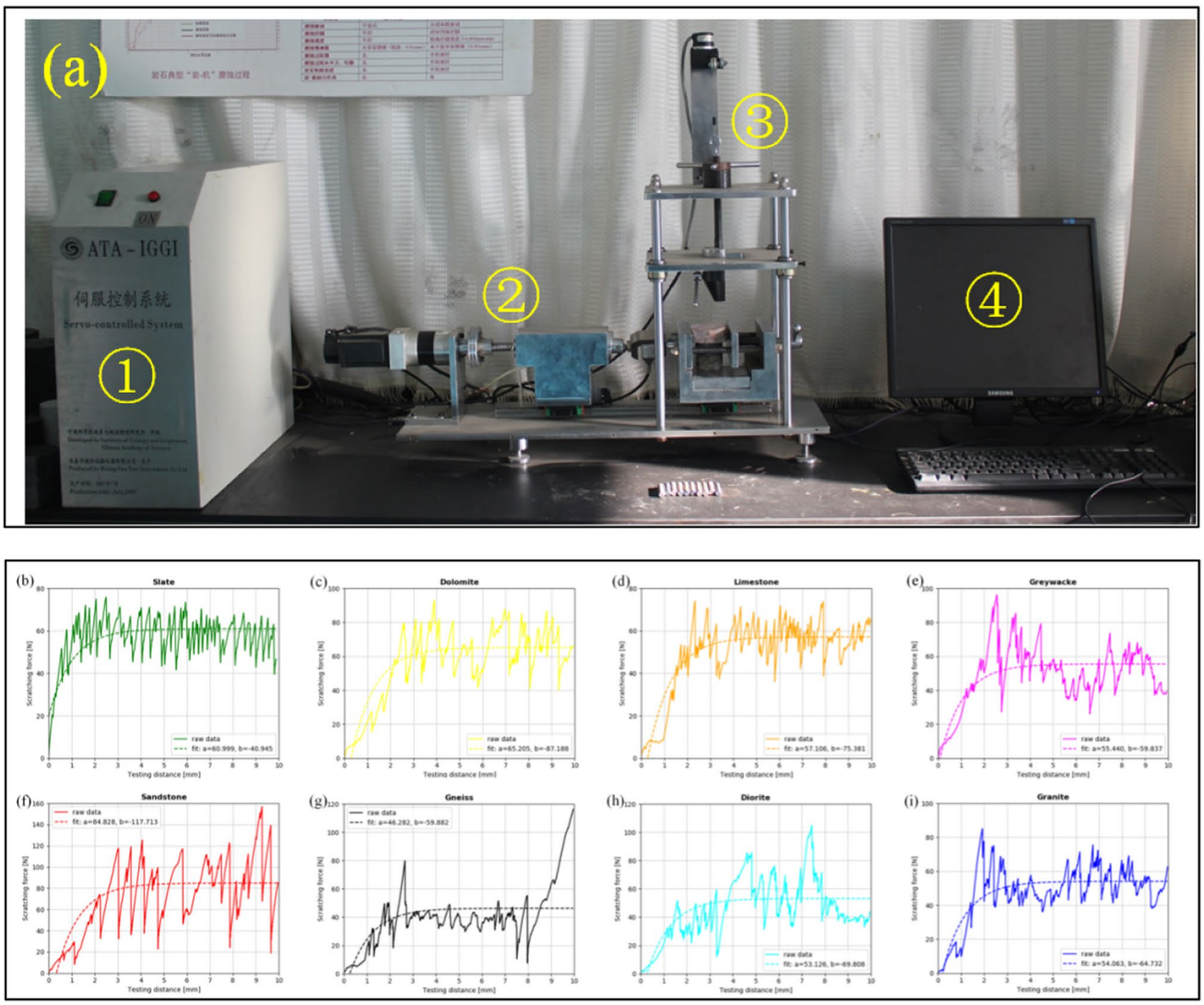

Fig. 9 **a** View on a modified Cerchar testing device (① Servo-controlled system; ② Horizontal loading-displacement sensor; ③ West apparatus; ④ Computer wit installed program) used to measure the applied force in scratching **b** Slate (MSF = 61 N); **c** Dolomite (MSF = 65 N); **d** Limestone (MSF = 57 N); **e** Greywacke (MSF = 55 N); **f** Sandstone (MSF = 85 N); **g** Gneiss (MSF = 46 N); **h** Diorite (MSF = 53 N); **i** Granite (MSF = 54 N) (Coloured fluctuated lines indicate the recorded scratching force, and the corresponding best-fitting lines indicate the calculated mean scratching force) (Zhang et al. 2020c; Zhang et al. 2021, modified)

70%, occurs within the initial first 1 mm of testing distance, 85% of wear is reached after 2 mm distance, and only 15% attributed to the final 8 mm. This finding was confirmed by Plinninger et al. (2003), who further emphasized that there is negligible variation in CAI when testing distances fall within 9.5–10.5 mm, and any extension of the testing distance is deemed unnecessary according to their results. However, Yarali et al. (2013) and Yarali and Duru (2016) presented a different perspective on this matter. They contended that the established testing distance may not be adequate. Their research indicated that a substantial portion, approximately 60%–70%, of the final CAI value is already achieved within the initial 2 mm of scratching, and this percentage gradually increases with diminishing returns up to 16 mm, eventually plateauing to 20 mm. Moreover, they found that nearly 85%–90% of the final CAI value can be reached at 10 mm, but it takes extending the testing distance to 15 mm to approach 99% of the final CAI value. Consequently, they proposed extending the testing distance to 15 mm to obtain a more accurate CAI value.

Plinninger et al. (2004) stated that scratching velocity has a limited effect on CAI values. Rostami et al. (2014) investigated the potential effect of scratching velocity on CAI, but no obvious correlation was found under various testing conditions. However, it should be noticed that rapid scratching velocity (e.g., 10 mm/s with Cerchar apparatus) may

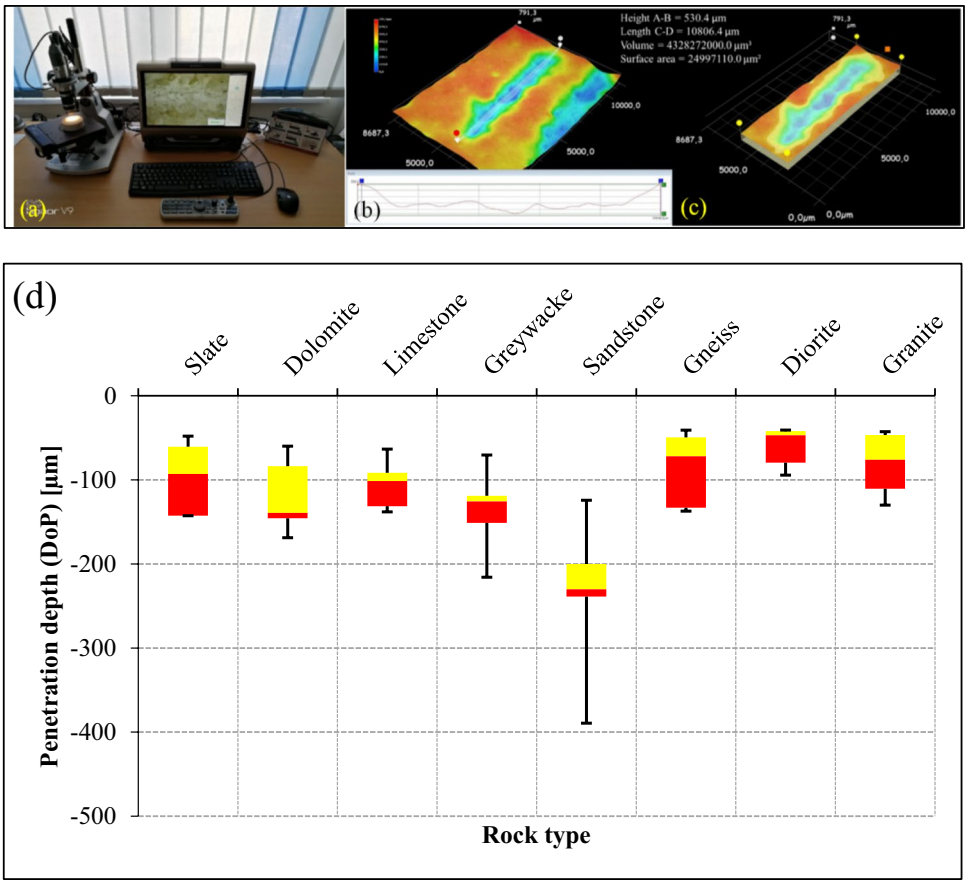

Fig. 10 **a** View on the digital microscope used to measure **b** The penetration depth and **c** Material removal volume for a sandstone sample; **d** Measurement results of penetration depth within different types of rocks (Zhang 2020, modified)

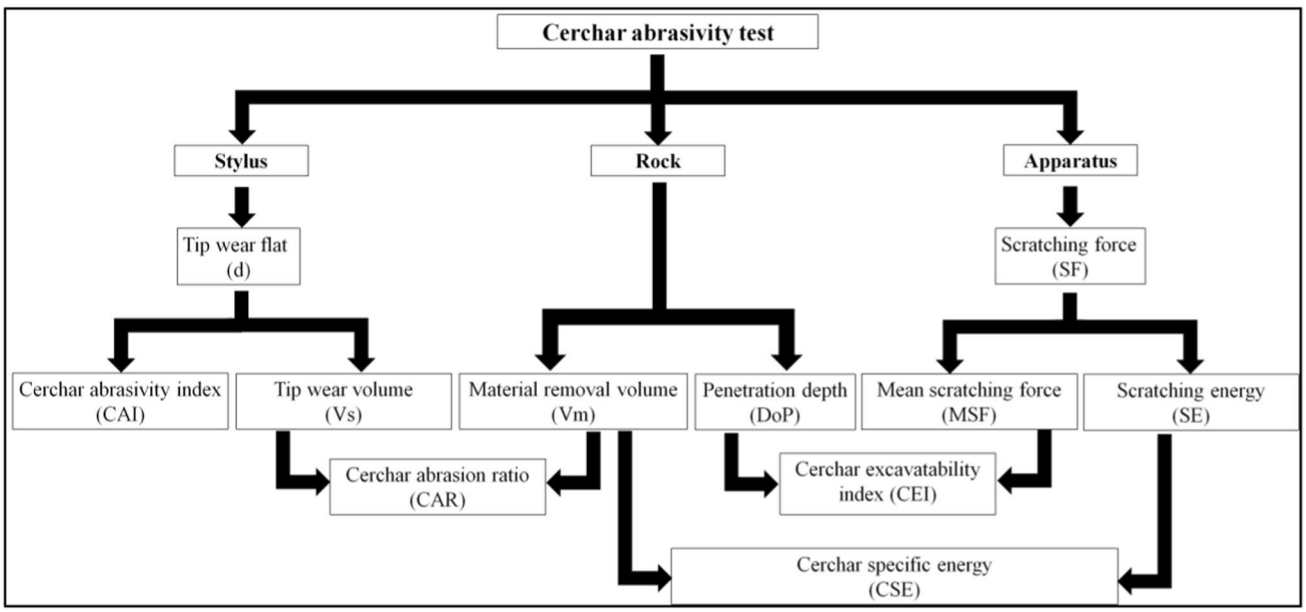

Fig. 11 Flowchart for determining and calculating the Cerchar abrasive parameters (e.g., abrasivity index, abrasion ratio, specific energy and excavatability index) (Zhang 2020, modified)

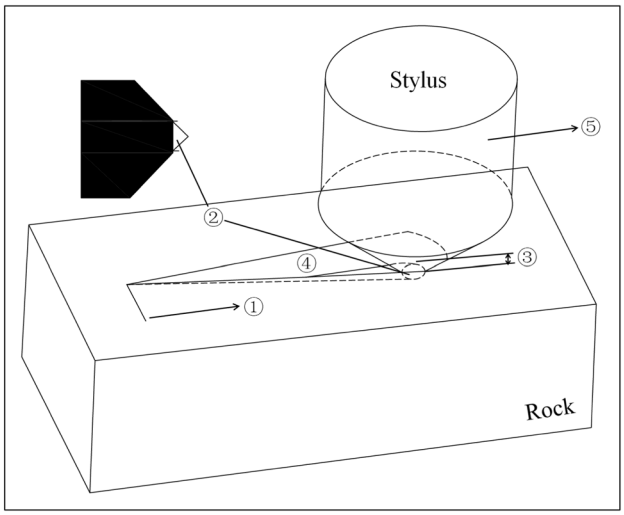

Fig. 12 Schematic diagram for determining the basic Cerchar abrasive parameters (① Scratching distance; ② Tip wear flat or volume; ③ Penetration depth; ④ Rock material removal; ⑤ Scratching force) (Rossi et al. 2020, modified)

lead to unintended stylus jumps from the sample surface, especially on rough rock surfaces. For West apparatus, a minimum velocity of 1 mm/s is required for offering a better control of the stylus.

3.6 Tip wear measurement

The accuracy of CAI, independent of operator skills, hinges primarily on the measurement approach on the abraded tip. When using the side-view method, Cerchar (1986) and Alber et al. (2014) recommended measuring the width of wear flat four times during each 90° rotation of the stylus and averaging them, while ASTM D7625-10 (2010) suggested measuring the two perpendicular diameters of abraded flat area for each stylus. West (1989) recognized that an occasional burr may appear on the downstream side of the tip, and then suggested either removing it before measurement or ignoring it entirely. To ensure the proper 90° angle on the tip, Rostami et al. (2005) recommended that the tip should be reproduced before measurement, as illustrated in Fig. 16a. Käsling (2009) identified three tip wear shapes and emphasized that a straight and smooth wear area is expected when the rock exhibits homogeneity and isotropy. In cases of rounded or asymmetric tip wear, as shown in Fig. 15, the author stressed the necessity of repeating the test for validity. He also recommended measuring the wear from the tip apex in two perpendicular directions. Aydin (2019) added to this discussion by pointing out that the wear flat can be measured in different ways: vertically from the top-view, horizontally from the side-view, or as the average value from both perspectives, as shown in Fig. 16b.

3.7 Numbers of single tests

Cerchar (1986) suggested performing two to three single scratches for fine-grained homogeneous rocks and five or more scratches for rocks with grain size larger than 1 mm. In a similar vein, West (1989) emphasized that conducting five single tests provides a representative assessment. Suana and Peters (1982) found that grain size within the range of 50–100 µm does not have a significant effect on CAI. Lassnig et al. (2008) conducted a comparative study, examining CAI values measured after five and ten scratches. They observed that approximately three-fourths of the samples exhibited variations of less than 0.2 CAI, indicating that CAI is not particularly sensitive to grain size. Käsling (2009)

Table 4 Definition of Cerchar abrasive parameters and their applications (Zhang 2020, modified)

Parameters	Symbols and formulas	Applications
Scratching distance (mm)	$L_s = 10$	Raw data
Tip wear flat (mm)	d	Raw data
Cerchar abrasivity index (0.1 mm)	$\mathrm{CAI} = \frac{1}{n}\sum_{i=1}^{n}(d_i \bullet 10)$	Rock abrasiveness
Tip wear volume (mm^3)	$V_s = \frac{1}{3}\pi \bullet \left(\frac{d}{2}\right)^3$	Rock abrasiveness
Penetration depth/Depth of scratch (mm)	DoP	Raw data
Material removal volume (mm^3)	V_m	Raw data
Scratching force (N)	$\mathrm{SF} = a + b \bullet e^{(-L_s)}$	Best-fitting curve of raw data
Mean scratching force (N)	$\mathrm{MSF} \approx b$	"Scratching-dominant-state" in best-fitting curve
Scratching energy (N mm or mJ)	$\mathrm{SE} = \int_{0\,mm}^{10\,mm} \mathrm{SF} \bullet d(L_s)$	Rock excavatability
Cerchar specific energy (mJ/mm^3)	$\mathrm{CSE} = \frac{\mathrm{SE}}{V_m}$	Rock-tool interaction; Cutting efficiency
Cerchar abrasion ratio (mm^3/mm^3)	$\mathrm{CAR} = \log_{10}(\frac{V_m}{V_s})$	Rock-tool interaction; Cutting effectivity; Tool wear
Cerchar excavatability index (N/mm)	$\mathrm{CEI} = \frac{\mathrm{MSF}}{\mathrm{DoP}}$	Rock excavatability

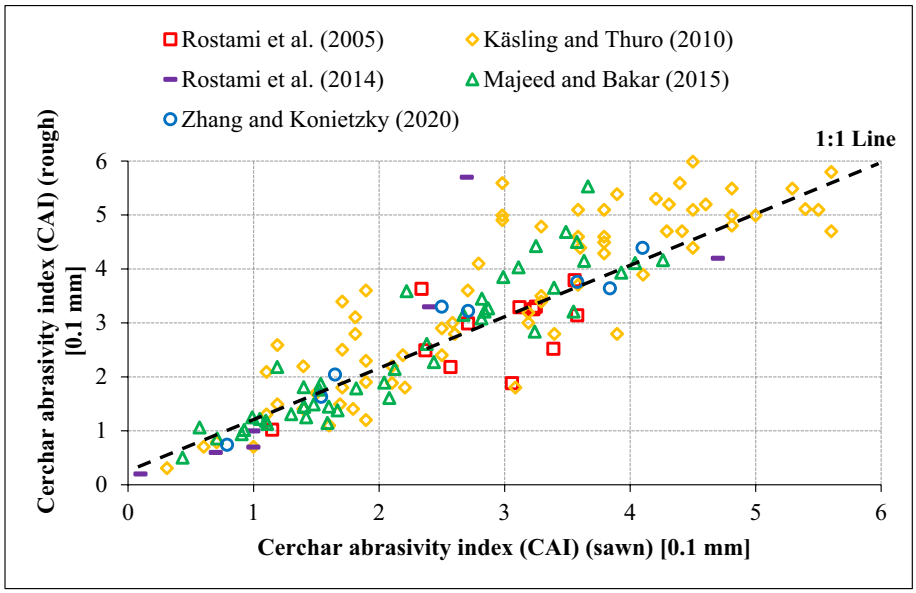

Fig. 13 CAI comparisons under rough vs. sawn rock surface conditions using HRC 55 stylus (Rostami et al. 2005, 2014; Käsling and Thuro 2010; Majeed and Abu Bakar 2015; Zhang and Konietzky 2020, modified)

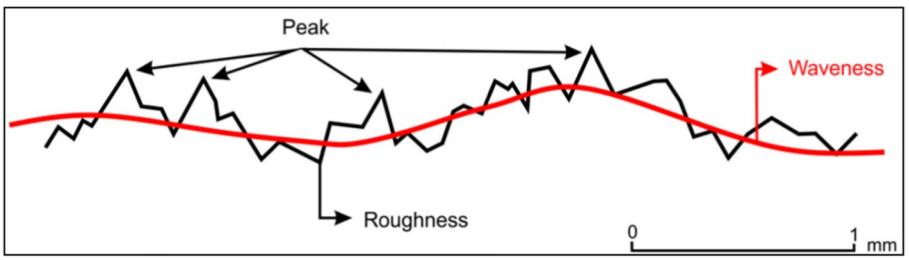

Fig. 14 Definition of roughness, waveness and peak number on a rough rock surface (Er and Tuğrul 2016)

delved further into the numbers of scratches required for reliable CAI assessment, considering rocks ranging from fine- to coarse-grained. The author concluded that the recommended five scratches may not suffice, especially for heterogeneous rocks. He suggested conducting 20–25 single tests to obtain a more accurate CAI value, as shown in Fig. 17.

3.8 Rock anisotropy

The Cerchar specification lacks explicit guidance on testing anisotropic rocks. To address this gap, Käsling et al. (2007) recommended a specific approach. They proposed performing Cerchar tests on stratified or foliated rocks (i.e., sedimentary and metamorphic rocks) three times to obtain the final CAI values. This entails ensuring that the sliding direction of the stylus is both orthogonal and parallel to the foliated surface, as well as sliding across the foliation surface of the rock sample. In line with this, the ISRM recommendation (Alber et al. 2014) advised scratching both orthogonal to and on the anisotropic surface of layered rock samples to obtain a more accurate CAI value. In a recent study, Zhang et al. (2020c) examined the dependency of CAI on rock anisotropy. They conducted Cerchar tests on two foliated metamorphic rocks (i.e., slate and gneiss), but no obvious correlation was found, as shown in Fig. 18.

3.9 Rock moisture

Regarding the rock moisture effect on CAI, Jacobs and Hagen (2009) pointed out that CAI decreases, as the rock moisture increases. Abu Bakar et al. (2016) found that the CAI values measured on saturated samples are generally lower than those on dry samples, with a factor of approximately 0.8. ASTM D7625-10 (2010) recommended measuring the actual water content of rock sample (e.g., as received, saturated, air dried, oven dried), when the Cerchar results are sensitive to it. Table 6 summarizes the testing condition-based factors influencing CAI.

Table 5 Chemical compositions of applied tool steels (Plinninger et al. 2003; Michalakopoulos et al. 2006; Jacobs and Hagen 2009; Käsling 2009; Stanford and Hagan 2009; Piazzetta et al. 2018; Zhang et al. 2020a)

Elements (Wt%)	Carbon (C)	Silicon (Si)	Manganese (Mn)	Chromium (Cr)	Vanadium (V)	Nickel (Ni)	Molybdenum (Mo)	Tungsten (W)	Phosphorus (P) <	Sulfur (S) <
EN24	0.36–0.44	0.1–0.4	0.45–0.70	1.0–1.4	–	1.3–1.7	0.20–0.35	–	0.035	0.04
Silver steel	0.95	0.25	1.1	0.55	0.1	–	–	0.55	–	–
H13	0.39	1.00	0.4	5.2	0.9	–	1.4	–	–	–
M340	0.54	0.45	0.4	17.3	0.1	–	1.1	–	–	–
Calmax	0.60	0.35	0.8	4.5	0.2	–	0.5	–	–	–
Sverker3	2.05	0.30	0.8	12.7	–	–	–	1.10	–	–
Rigor	1.00	0.30	0.6	5.3	0.2	–	1.1	–	–	–
S 600	0.90	0.25	0.3	4.1	1.8	–	5.0	6.40	–	–
AISI A2	0.994	–	–	4.57	0.115	–	–	0.98	–	–
115*CrV3*	1.10–1.25	0.15–0.30	0.2–0.4	0.5–0.8	0.07–0.12	–	–	–	0.030	0.03

4 Correlations between physical–mechanical parameters and CAI

4.1 Statistical analysis approach

In rock mechanics, three distinct statistical analysis approaches have been adopted for the correlation studies: (1) Conventional Statistical Analysis: The most common method involves single or multiple regression analysis, including R^2-statistic, Student's t-test and F-test (analysis of variance, ANOVA). This approach, based on the least squared estimation procedure, has found wide application in the Cerchar test (Al-Ameen and Waller 1994; Yarali et al. 2008; Khandelwal and Ranjith 2010; Deliormanli 2012; He et al. 2015; Ko et al. 2016; Capik and Yilmaz 2017; Torrijo et al. 2018; Ozdogan et al. 2018). Additionally, Student's t-test and ANOVA are frequently adopted when the correlation of determination (R^2) provides inadequate (Majeed and Abu Bakar 2015; Moradizadeh et al. 2016; Er and Tuğrul 2016; Cheshomi and Moradhaseli 2017; Teymen 2020); (2) Artificial Neutral Network Analysis (ANNA): This method involves the calculation of various statistical parameters for both measured and predicted values. However, ANNA necessitates training, validation and testing, often requiring a substantial number of rock samples for a robust result (Kahraman et al. 2010, 2015; Tripathy et al. 2015); (3) Gene Expression Programming (GEP): Recently, a GEP model, based on genetic algorithms, has emerged as a tool for establishing correlations between geotechnical parameters and rock abrasiveness (Kadkhodaei and Ghasemi 2019).

4.2 Rock mineralogy and petrography

Table 7 summarizes the rock mineralogical-petrographical characteristics influencing CAI. In the context of rock mineralogy and petrography, several parameters play a crucial role in assessing abrasiveness. These include the composition and content, size and shape of individual minerals, as well as types of cement materials present and their respective degrees of presence.

Quartz stands out as a mineral that exists in a wide range of rocks, including igneous, sedimentary and metamorphic rocks (e.g., granite, sandstone and quartzite). Consequently, it holds a position of dominance in affecting both rock strength and abrasiveness. Over time, numerous scholars have undertaken investigation into the correlation between rock abrasiveness and quartz-related parameters, such as size, shape, content and equivalence. Silica (SiO_2) emerges as an indicator of abrasiveness, because it not only reflects the quantity of quartz but also the presence

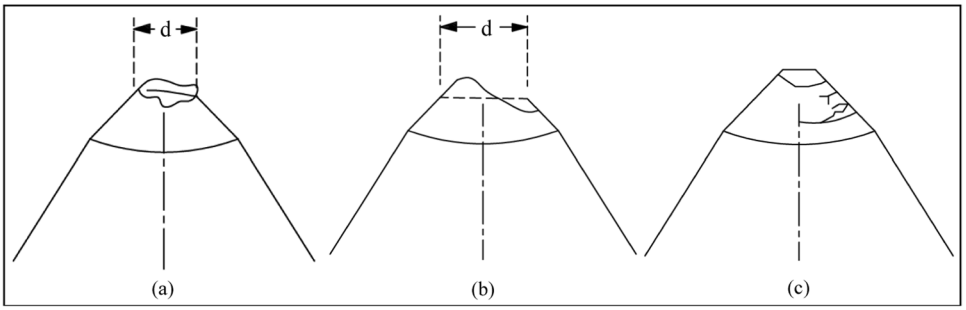

Fig. 15 Sketches of the abraded stylus tip: **a** Normal wear; **b** Non-symmetrical wear (Measuremet is still possible as an average of the value in two sides); **c** Very rough surface (Measurement is unsuitable, and a remade of test is necessary) (ASTM D7625-10 2010)

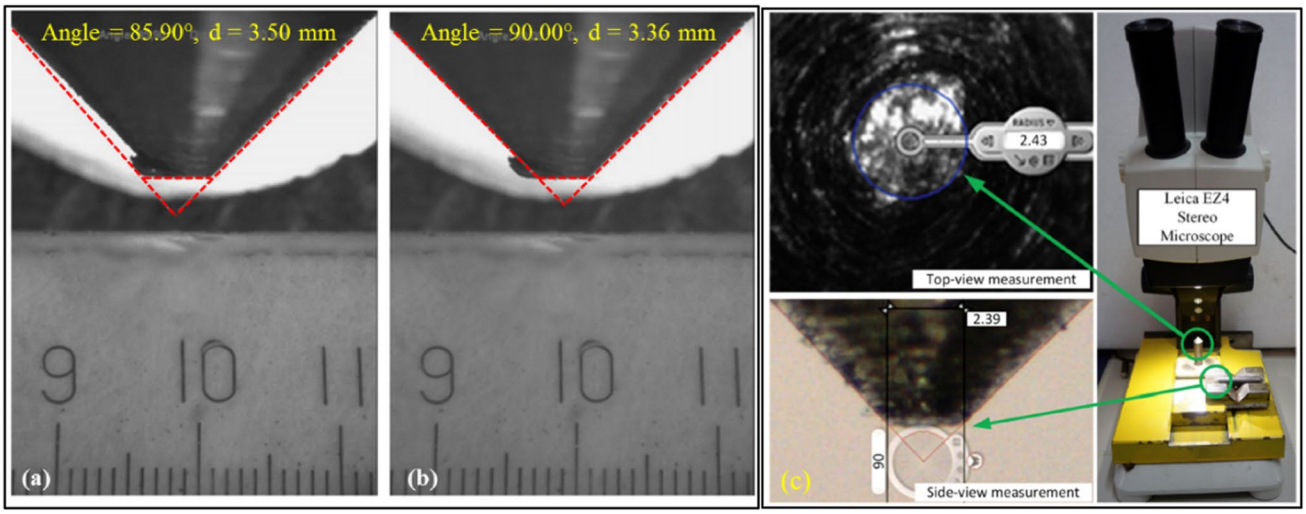

Fig. 16 Measurement of the tip wear: **a** Wear flat measurement with burr; **b** Wear flat measurement without burr; **c** Measurement in side-view method vs. top-view method (Rostami et al. 2005; Yarali and Duru; 2016; Aydin 2019)

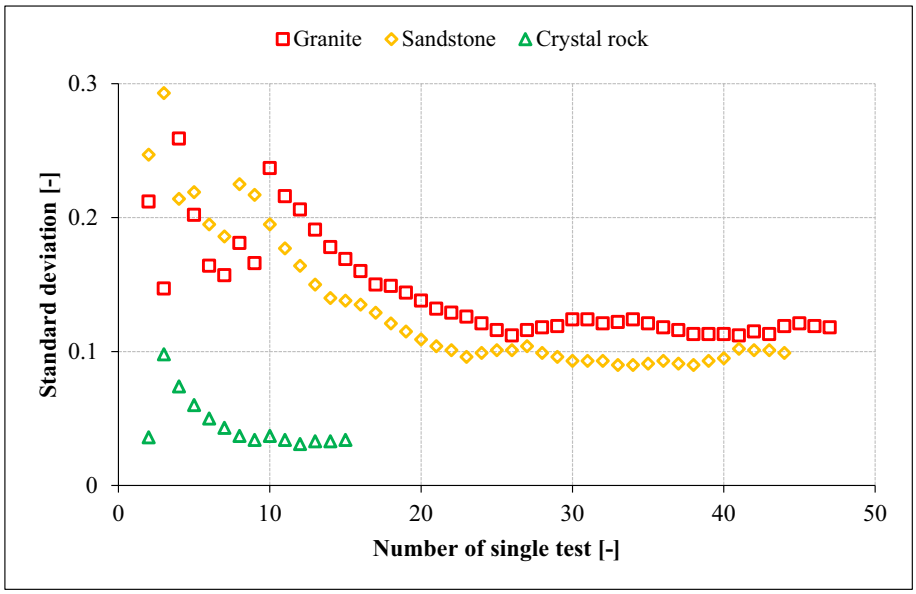

Fig. 17 Dependence of standard deviations in CAI on numbers of single tests (Käsling et al. 2007, modified)

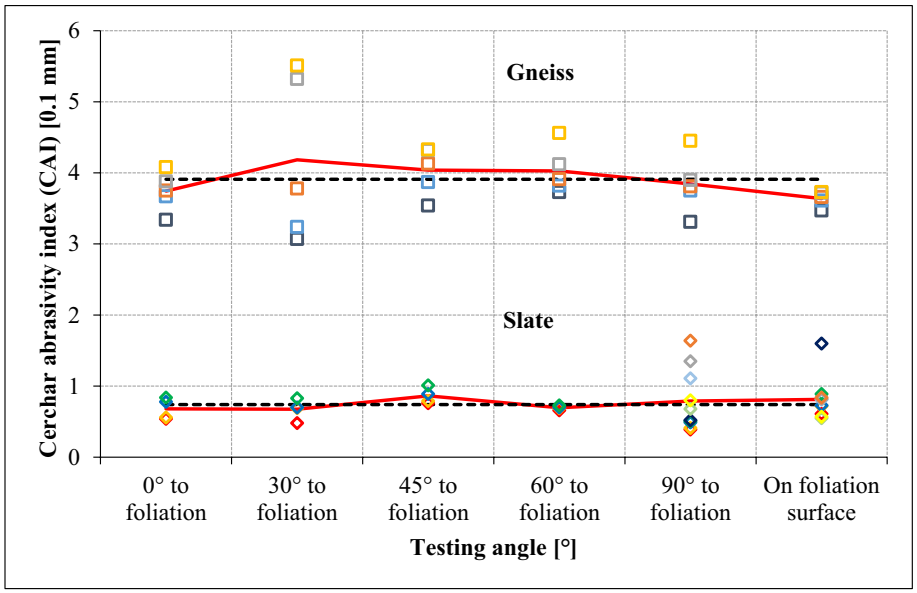

Fig. 18 Effect of rock anisotropy on CAI (red solid lines indicate the mean CAI calculated from one single test, and black dash lines indicate the final CAI value calculated from all single tests) (Zhang et al. 2020c, modified)

of silicate minerals like feldspars, micas and clay minerals. When quartz assumes a dominant role as the abrasive mineral, the quartz content (C_{Qtz}) serves as an effective predictor of abrasiveness. Experimental findings have consistently demonstrated that rock abrasiveness increases, as the quartz content increases (West 1986a). It is worth noting that, in the context of mineral hardness, tool steel registers at approximately 5.5 on the Mohs hardness scale, and minerals surpassing this value are generally considered abrasive. Therefore, in addition to quartz with a Mohs hardness number of 7, other minerals like fluorite, apatite, orthoclase and feldspar, falling within the Mohs hardness range of 4 to 6, possess the potential for abrasive. Besides quartz content, the equivalent quartz content (EQC) is another crucial parameter reflecting not only the mineral compositions but also the rock hardness, and thereby affecting abrasiveness. The EQC is calculated by multiplying the percentage of individual minerals by their respective Rosiwal hardness number (Thuro 1996). Similar to the quartz content, scholars have extensively investigated the relationship between CAI and EQC, and a great variety of correlations from linear to non-linear, from bivariate to multivariate has been established, depending on the specific types of rocks considered and the quantity of rock samples examined (Suana and Peters 1982; West 1986a; Yarali et al. 2008; Thuro and Käsling 2009; Moradizadeh et al. 2016; Capik and Yilmaz 2017). Fig. 19 shows these CAI-EQC correlations for various types of rocks. Notably, for igneous rocks, including both extrusive and intrusive varieties, CAI tends to increase with higher EQC values. A similar positive correlation is observed for metamorphic rocks. However, classic sedimentary rocks like mudstone, siltstone, sandstone, breccia and conglomerate exhibit substantial fluctuations in CAI-EQC correlations, attributable their geological origins. Conversely, chemical sedimentary rocks like limestone, dolomite and marble do not exhibit an obvious correlation, likely due to the rarity of hard and abrasive minerals within these rocks.

McFeat-Smith and Fowell (1977) underscored that assessing rock abrasiveness solely based on quartz content is inadequate, as it hinges on the presence and composition of cement materials. Al-Ameen and Waller (1994) reinforced this viewpoint by suggesting that CAI values obtained from coarse-grained rocks primarily reflect the abrasive nature of individual minerals, rather than the overall rock composition. Such statements are worth considerable, because the testing distance is fixed at 10 mm, amplifying the influence of grain size, shape and cement materials on the test results. For instance, in the case of coarsely heterogeneous crystalline rocks like granite, porphyry and gneiss, the abrasivity index predominantly mirrors the hardness of individual minerals (e.g., quartz or feldspar) when these minerals are scratched among large, inter-locked mineral grains. However, in sedimentary rocks like sandstone, siltstone or mudstone, which are relatively fine-grained and homogeneous, the types of cement materials (e.g., clayey, siliceous, carbonate or ferritic) and their degrees of cementation exert a more dominant influence on the test results (Yarali et al. 2008). Figure 20 represents two major observations: (1) Sedimentary rocks with siliceous cement exhibit a higher abrasive potential; (2) An increase in the degree of cementation correlates with higher abrasiveness.

To study the grain size and shape effect on rock abrasiveness, He et al. (2015) proposed a comprehensive parameter known as microstructure coefficient, which is defined as the ratio of size coefficient to the shape coefficient, and then

Table 6 Summary of testing condition-based factors influencing CAI

Factors	Standards	Conclusions	References
Test apparatus	Cerchar or West	West apparatus is more stable	Käsling et al. (2007)
		Automatic testing device can better control the testing distance and velocity	Sotoudeh et al. (2014)
Applied load	7 kg weight	$CAI = 0.1333 \cdot F_N + 0.4044$ (HRC = 15)	Jacobs and Hagan (2009)
		$CAI = 0.0144 \cdot F_N + 2.1442$ (HRC 40–42)	Ghasemi (2010); Rostami et al. (2014)
		$CAI = 0.0087 \cdot F_N + 2.047$ (HRC 54–56)	
Stylus metallurgy	Steel with 2000 MPa tensile strength	115CrV4 tool steel is heat treated to *HRC* 55	Plinninger et al. (2003)
		CAI does not change using different tool steels as long as hardness is identical	Standford and Hagan (2009)
		$CAI_{CrNiMo\text{-}Steel} = 1.037 \cdot CAI_{CrV\text{-}Steel}$	Käsling (2009)
Stylus hardness	HRC 54–56 (HRC 40–42)	$CAI_{55} = 0.587356 \cdot CAI_{40} + 0.110914$	Michalakopoulos et al. (2006)
		$CAI_{Hv220} = 1.46 \cdot CAI_{Hv660} + 1.29$ (H_{V220} = HRC 55, H_{V660} = HRC 15)	Fowell and Abu Bakar (2007)
		$CAI = -0.0766 \cdot HRC + 5.8044$ (Sandstone)	Stanford and Hagan (2009)
		$CAI_{55} = 0.705 \cdot CAI_{40}$	Käsling and Thuro (2010)
Surface condition	Rough	$CAI(EN3)_{rough} = CAI(EN3)_{sawn} - 0.01$	Al-Ameen and Waller (1994)
		$CAI_{rough} = 0.99 \cdot CAI_{sawn} + 0.48$	Plinninger et al. (2003); ASDM D7625-10 (2010)
		$CAI_{sawn} = 0.878 \cdot CAI_{rough}$	Käsling and Thuro (2010)
		$CAI_{rough} = 1.1683 \cdot CAI_{sawn} - 0.2186$	Yarali and Duru (2016)
		$CAI = 0.52 \cdot R + 3.67$	Er and Tuğrul (2016)
		$CAI = 0.03 \cdot W + 2.12$	
		$CAI = 0.08 \cdot N_{Peak} + 4.19$	
Testing distance	10 mm	Lengthening is not necessary	Plinninger et al. (2003); Zhang et al. (2020c)
		$CAI_{15\ mm} = 1.0442 \cdot CAI_{10\ mm} + 0.1199$	Yarali et al. (2013); Yarali and Duru (2016)
Scratching CAIHR-CASTM velocity	1 mm/s or 10 mm/s	No dependence	Rostami et al. (2014); Zhang et al. (2020c)
Numbers of single tests	5 scratches	20–25 single scratches are more suitable	Käsling et al. (2007); Käsling (2009)
Tip wear measurement	4 times with each 90° rotation	Burr on the downstream side of the wear flat must be removed. Reproduce the correct angle before measuring	West (1989); Rostami et al. (2005); Käsling (2009)
Rock anisotropy	N.A	Although no dependence is found, at least scratches orthogonal to and on the anisotropic surface of layered rocks should be done	Käsling (2009); Alber et al. (2014)
Rock moisture (%)	Natural	$CAI = -0.2612 \cdot M + 3.0676$	Jacobs and Hagen (2009)
		$CAI_{sat} = 0.782 \cdot CAI_{dry} + 0.128$	Abu Bakar et al. (2016)

related it to CAI. While individual textural and mechanical parameters showed only weak correlations with CAI, more robust associations emerged when considering complex mechanical-mineralogical-petrographical parameters. This reaffirms the notion that abrasiveness is inherently linked to the mechanical and mineralogical properties of rocks. Ündül and Er (2017) delved into the influence of Ferret's diameter (Howarth and Rowlands 1987) and the perimeter

Table 7 Summary of rock mineralogical-petrographical characteristics influencing CAI (bivariate)

Parameters	Models	References	Remarks
Silica/Aluminum (SiO_2/Al_2O_3) (%)	$CAI = 0.0448 \cdot SiO_2 - 0.0886$	Torrijo et al. (2018)	73 andesitic samples
	$CAI = -0.0749 \cdot Al_2O_3 + 3.5651$		
Quartz content (C_{Qtz}) (%)	$CAI = 0.0336 \cdot C_{Qtz} - 0.6825$	West (1986a)	31 coal sediments
	$CAI = 0.0309 \cdot C_{Qtz} - 0.0795$	Yarali et al. (2008)	29 coal sediments
	$CAI = 0.0489 \cdot C_{Qtz} - 1.2909$		29 coal sediments without mudstone
	$CAI = 1.229 \cdot e^{0.014 \cdot C_{Qtz}}$	Moradizadeh et al. (2016)	10 sandstones
	$CAI = 0.055 \cdot C_{Qtz} + 1.06$		8 metamorphic rocks
	$CAI = 0.02 \cdot C_{Qtz} + 4.74$	Er and Tuğrul (2016)	12 granitic rocks
Equivalent quartz content ($EQC = \sum_{i=1}^{n} A_i \cdot R_i$) (%)	$CAI = 0.0313 \cdot EQC - 0.1619$	Yarali et al. (2008)	29 coal sediments
	$CAI = 0.052 \cdot EQC - 1.5769$		29 coal sediments without mudstone
	$CAI = 0.0537 \cdot EQC$	Thuro and Käsling (2009)	52 datasets
	$CAI = 0.039 \cdot EQC + 1.241$	Moradizadeh et al. (2016)	All 36 rock samples
	$CAI = 1.178 \cdot e^{0.015 \cdot EQC}$		10 sandstones
	$CAI = 2.679 \cdot e^{0.008 \cdot EQC}$		6 plutonic rocks
	$CAI = 0.056 \cdot EQC + 0.728$		8 metamorphic rocks
	$CAI = 0.0644 \cdot EQC + 0.5485$	Capik and Yilmaz (2017)	43 rock samples
	$CAI = 0.04 \cdot EQC + 0.99$	Cheshomi and Moradhaseli (2017)	Granite, Gabbro, Hornfels
Quartz grain size (d_{Qtz}) (mm)	$CAI = 2.7928 \cdot d_{Qtz} + 0.6677$	Yarali et al. (2008)	29 coal sediments
	$CAI = 1.47 \cdot d_{Qtz} + 4.52$	Er and Tuğrul (2016)	12 granitic rocks
Feldspar content (C_{Fsp}) (%)	$CAI = 0.0305 \cdot C_{Fsp} + 0.6360$	Torrijo et al. (2018)	73 andesitic CAI samples
Feldspar grain size (d_{Fsp}) (mm)	$CAI = 1.8243 \cdot d_{Fsp} + 0.4447$		
Cement degree (CD) (%)	$CAI = 0.0705 \cdot CD - 1.612$	Yarali et al. (2008)	29 coal sediments
Microstructure coefficient (–)	Positive correlation	He et al. (2015)	20 rock samples
Ferret's diameter ($F_{Ø}$) (mm)	$CAI = -2.3346 \cdot F_{ØPlgFsp} + 4.3221$	Ündül and Er (2017)	23andesites and rhyodacites
	$CAI = -3.149 \cdot F_{Øopa} + 3.929$		
Perimeter (P) (mm)	$CAI = -1.006 \cdot P_{PlgFsp} + 4.4504$		
	$CAI = -1.102 \cdot P_{Opa} + 3.85$		

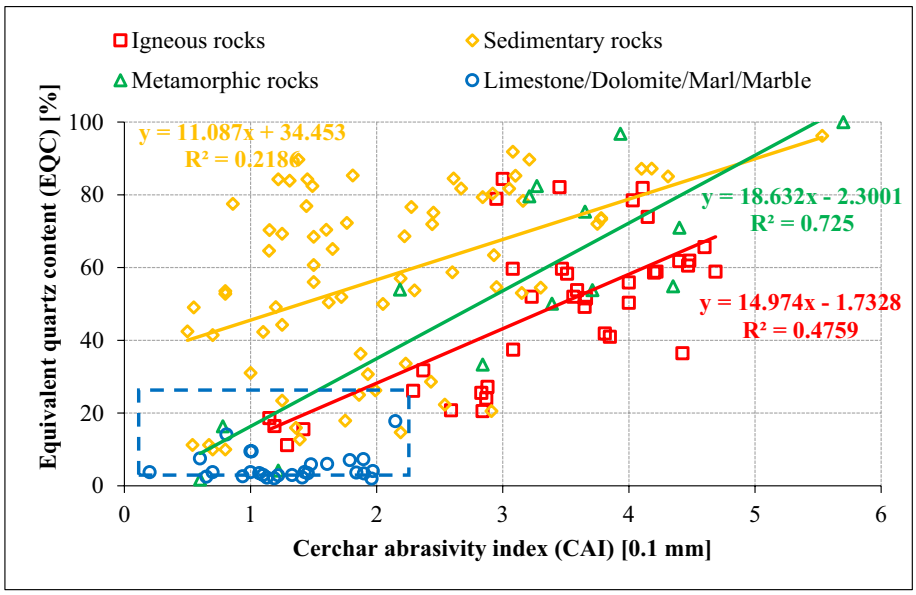

Fig. 19 Correlations between CAI and EQC (Yarali et al. 2008; Rostami et al. 2014; He et al. 2015; Moradizadeh et al. 2016; Capik and Yilmaz 2017, modified)

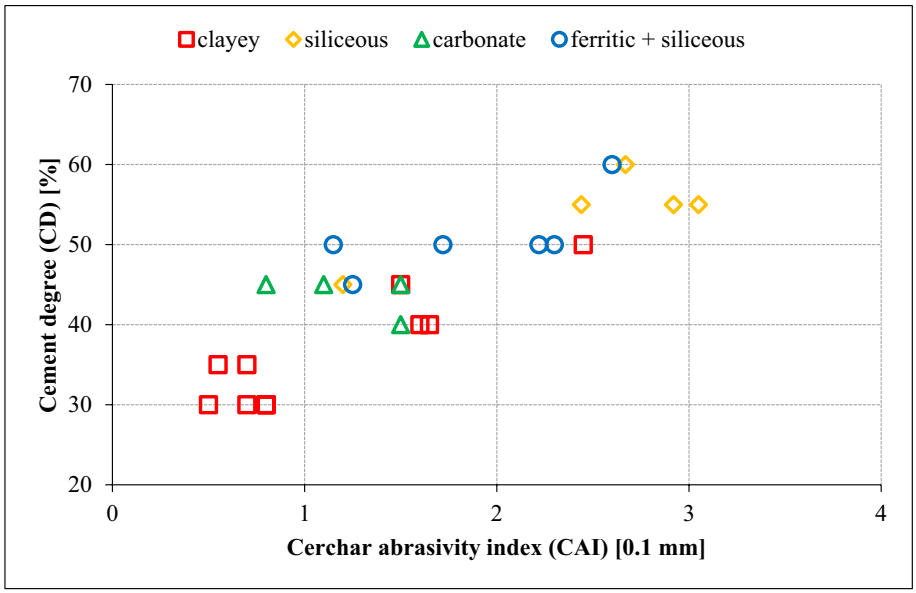

Fig. 20 Correlations between CAI and CD (Yarali et al. 2008, modified)

Table 8 Summary of rock strength properties influencing CAI (bivariate)

Parameters	Models	References	Remarks
Uniaxial compressive strength (UCS) (MPa)	$CAI(EN3) = -0.0001 \cdot UCS^2 + 0.05 \cdot UCS - 1.38$	Al-Ameen and Waller (1994)	–
	$UCS = 54.47 \cdot CAI + 18.26$	Deliormanli (2012)	15 marbles
	$CAI = 0.02 \cdot UCS + 3.19$	Er and Tuğrul (2016)	12 granitic rocks
	$CAI = 0.0189 \cdot UCS + 0.177$	Capik and Yilmaz (2017)	43 samples
	$CAI = 0.0059 \cdot UCS + 1.949$	Ündül and Er (2017)	23 andesites and rhyodacites
	$UCS = 51.82 \cdot CAI - 31.58$	Teymen (2020)	80 samples
Young's modulus (E) (GPa)	$CAI = 0.0372 \cdot E + 1.4804$	Ündül and Er (2017)	23 andesite and rhyodacite
	$E = 4.84 \cdot CAI^{1.32}$	Teymen (2020)	80 samples
Brazilian tensile strength (BTS) (MPa)	$CAI = 0.11 \cdot BTS + 3.73$	Er and Tuğrul (2016)	12 granitic rocks
	$CAI = 0.1538 \cdot BTS + 0.0247$	Capik and Yilmaz (2017)	43 samples
	$CAI = 0.1069 \cdot BTS + 1.6583$	Ündül and Er (2017)	23 andesites and rhyodacites
	$BTS = 2.8 \cdot CAI^{1.086}$	Teymen (2020)	80 samples
Point load strength (Is_{50}) (MPa)	$CAI = 1.393 \cdot e^{0.089 \cdot Is_{50}}$	Moradizadeh et al. (2016)	10 sandstones
	$CAI = 0.159 \cdot Is_{50} + 0.61$		8 limestones
	$CAI = 0.2393 \cdot Is_{50} + 0.3446$	Capik and Yilmaz (2017)	43 samples
	$Is_{50} = 1.33 \cdot e^{0.475 \cdot CAI}$	Teymen (2020)	80 samples
Direct shear strength (DSS) (MPa)	$DSS = 7.72 \cdot CAI + 2.87$	Deliormanli (2012)	15 CAI marbles
P-wave velocity (v_p) (km/s or m/s)	$CAI = 0.0009 \cdot v_p + 1.9375$	Khandelwal and Ranjith (2010)	13 rocks
	$CAI = 0.58 \cdot v_p + 2.55$	Er and Tuğrul (2016)	12 granitic rocks
	$CAI = 0.938 \cdot v_p - 1.103$	Ündül and Er (2017)	23 andesites and rhyodacites
Porosity (n) (%)	Increased CAI per MPa confinement $= 0.0094 \cdot n + 0.0131$	Alber (2008)	sandstone; greywacke; granite; micaschist

of individual mineral grains on CAI, based on two volcanic rocks. Experimental results revealed that in the case of feldspars and opaque minerals, simple correlations can effectively capture their relationship with CAI. Moreover, in feldspar-rich rocks, the content and grain size of feldspar exhibit similar behaviour to quartz, both contributing significantly to rock abrasiveness (Torrijo et al. 2018).

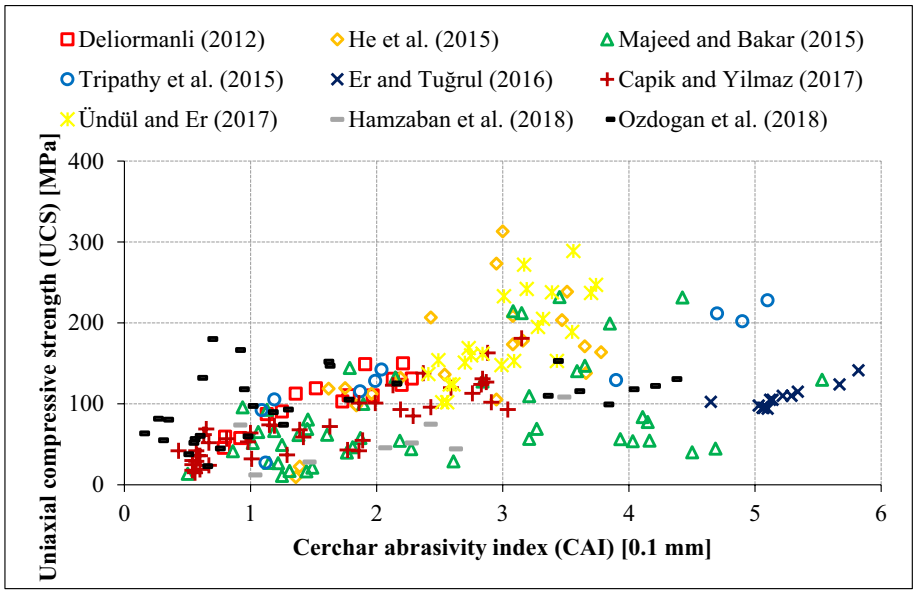

Fig. 21 Correlations between CAI and UCS (Deliormanli 2012; He et al. 2015; Majeed and Abu Bakar 2015; Tripathy et al. 2015; Er and Tuğrul 2016; Capik and Yilmaz 2017; Ündül and Er 2017; Hamzaban et al. 2018; Ozdogan et al. 2018, modified)

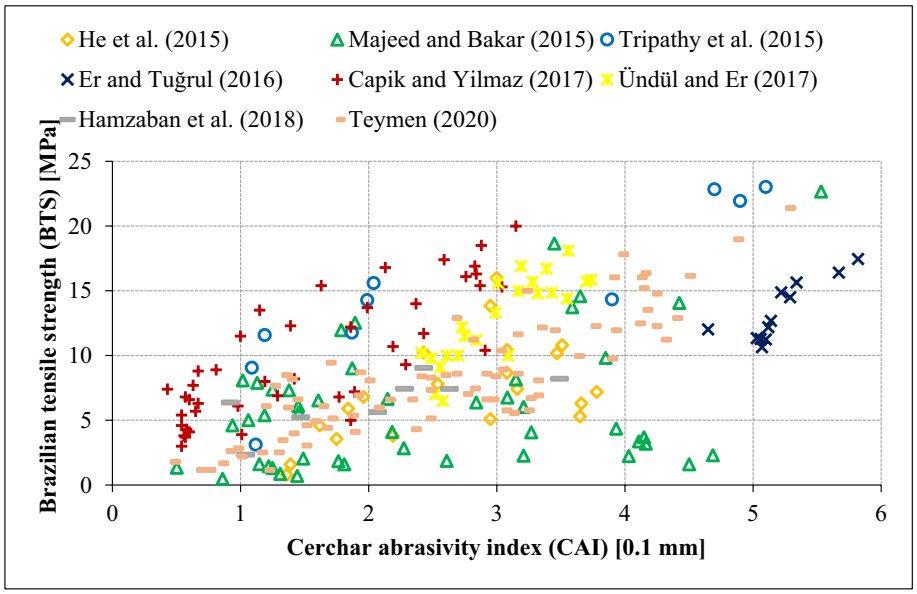

Fig. 22 Correlations between CAI and BTS (He et al. 2015; Majeed and Abu Bakar 2015; Tripathy et al. 2015; Er and Tuğrul 2016; Capik and Yilmaz 2017; Ündül and Er 2017; Hamzaban et al. 2018; Teymen 2020, modified)

4.3 Rock strength property

Table 8 summarizes the rock strength properties influencing CAI. Among the various physical-mechanical properties of rocks, compressive strength stands out as a dominant parameter affecting rock abrasiveness. Al-Ameen and Waller (1994) established a connection between CAI and uniaxial compressive strength (UCS), highlighting that even in cases where rocks lack abrasive minerals, CAI maintains a strong correlation with UCS. Kahraman et al. (2010) and Kahraman et al. (2015) further affirmed the feasibility of linking CAI to einaxial and triaxial strengths of tectonic rocks. Ündül and Er (2017) and Teymen (2020) found that Young's modulus (E) exclusively relates to CAI for intact rocks. The point load index (Is_{50}) also exhibits a direct association with CAI (Moradizadeh et al. 2016; Teymen 2020). Figures 21, 22 and 23 illustrate the pronounced positive correlations between CAI and UCS, BTS and Is_{50}, respectively, as observed by numerous scholars.

For decades, two fundamental rock cutting theories have been developed based on rock failure modes: the tension-induced failure mode (Evans 1958) and the shear-induced failure mode (Nishimatsu 1972). Evans' theory describes the penetration of a wedge-shaped tool into the buttock of rock, while Nishimatsu's cutting model relies on the Mohr-Coulomb criterion to explain chip formation in stressed

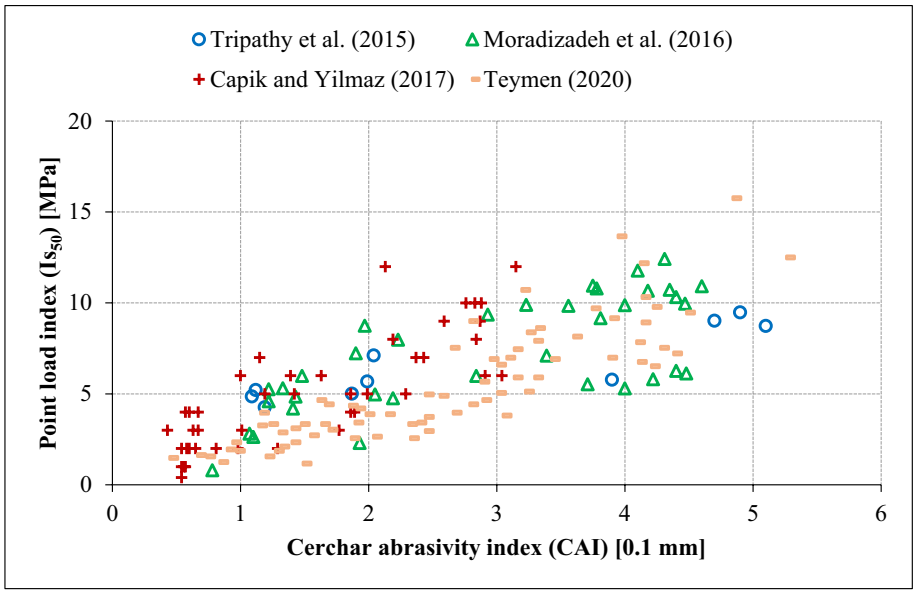

Fig. 23 Correlations between CAI and Is_{50} (Tripathy et al. 2015; Moradizadeh et al. 2016; Capik and Yilmaz 2017; Teymen 2020, modified)

conditions. Therefore, stylus scratching can be seen as a process that overcomes either the shear strength, tensile strength, or both, leading to rock fracture and damage. Experimental findings demonstrated that both direct shear strength (DSS) and Brazilian tensile strength (BTS) can be linked to CAI (Deliormanli 2012).

Ultrasonic measurements are frequently used to determine the velocity of elastic waves within rocks. Using P-wave velocity (v_p), the quality of rocks can be estimated non-destructively. Khandelwal and Ranjith (2010) found that P-wave velocity exhibits a strong correlation with CAI, suggesting that compact rocks possess higher abrasive potential compared to porous rocks. Ündül and Er (2017) highlighted that v_p stands out as the most reliable parameter for CAI determination, surpassing UCS, E and BTS.

Contrary to some expectations, Alber (2008) concluded that the porosity (n) does not significantly affect rock abrasiveness. It primarily reflects how easily tools plow through rocks without causing substantial wear, particularly in the presence of numerous pores. However, Ozdogan et al. (2018) achieved a more robust multivariate association by linking abrasiveness to porosity.

4.4 Rock hardness and abrasiveness

Table 9 summarizes the rock hardness and abrasiveness influencing CAI. In mineralogy, hardness stands out as a defining property of mineral. It is not a fundamental physical quantity, but can be related to the local strength of rock (Atkinson 1993). Geologist and mineralogist typically approach the quantification of rock hardness by initially determining the mineral composition and subsequently computing composite hardness based on mineral constituents. Three fundamental hardness scales have been established: Mohs scratch hardness scale (H_M), Rosiwal grinding hardness scale (H_R) and Vickers indentation hardness scale (H_V) (Rosiwal 1916).

West (1989) demonstrated a linear correlation between CAI and H_M, supported by an analysis of six minerals. More recently, Kaspar et al. (2023) introduced a polynomial correlation between CAI and H_V, as shown in Fig. 24. To represent rock hardness, various indexes have been proposed, including abrasive mineral content (AMC), equivalent quartz content (EQC) (West 1981) and Vickers hardness number of rock (VHNR) (Bruland 1998). These indexes correspond to the Mohs, Rosiwal, and Vickers hardness scales, respectively.

In rock mechanics and engineering, an array of laboratory testing methods has emerged to ascertain rock hardness, categorized as indentation method and rebound method. While Brinell, Rockwell, Vickers and Knoop hardness tests fall under the indentation methods, Shore scleroscope hardness (SSH) and Schmidt hammer hardness (SHH) tests are regarded as rebound methods. The hardness of rock is closely tied to its local strength against tool indentation, with abrasive wear primarily contingent on the proportion of hard mineral constituents within the rock, especially their size, shape and angularity. Notably, correlations between rock abrasiveness and hardness, as expressed by the Shore scleroscope and Schmidt hammer tests, have been established (Capik and Yilmaz 2017; Ozdogan et al. 2018).

Besides the Cerchar index, several geotechnical parameters have been developed to present the abrasive potential of rocks. These parameters measured based on the laboratory tests include NTNU abrasion value (AV or AVS) (Selmer-Olsen and Lien 1960), LCPC abrasivity

Table 9 Summary of rock hardness and abrasiveness influencing CAI (bivariate)

Parameters	Models	References	Remarks
Mohs hardness number (H_M) (–)	Positive linear correlation	West (1989)	6 minerals
Abrasive mineral content (AMC = $\sum_{i=1}^{n} A_i \bullet H_{Mi}$) (–)	AMC = 0.1539• + 0.3773	Hamzaban et al. (2014)	17 samples
Equivalent quartz content (EQC) (%)	See Table 7		
Vickers hardness number (H_V) (kgf/mm^2)	$H_V = 20.404 \bullet CAI^2 + 67.017 \bullet CAI + 27.098$	Kaspar et al. (2023)	10 minerals
Vickers hardness number of rock (VHNR = $\sum_{i=1}^{n} A_i \bullet H_{Vi}$) (%)	–	–	–
Knoop hardness number (H_K) (N/mm^2)	$H_K = 47.269 \bullet CAI + 83.046$	Figarska-Warchoł and Rembiś (2021)	11 sandstone samples
Shore scleroscope hardness (SSH) (N/mm^2)	CAI = 0.04•SSH + 1.87	Er and Tuğrul (2016)	12 granitic rocks
	CAI = 0.06359•SSH – 2.562	Ozdogan et al. (2018)	30 samples
Schmidt hammer hardness (SHH) (N/mm^2)	CAI = 0.04•SHH + 2.73	Er and Tuğrul (2016)	12 granitic rocks
	$CAI = 0.0811 \bullet SHH_{L\text{-type}} - 2.3246$	Capik and Yilmaz (2017)	43 samples
	$CAI = 0.0787 \bullet SHH_{N\text{-type}} - 2.1913$		
Böhme abrasion (BA) (cm^3/50 cm^2)	BA = – 4.64•CAI + 25.06	Deliormanli (2012)	15 marbles
	CAI = – 0.1•BA + 6.9	Er and Tuğrul (2016)	12 granitic rocks
	$BA = 55.2 \cdot CAI^{-1.16}$	Teymen (2020)	80 samples
Wide wheel abrasion (WWA) (mm)	WWA = – 1.96•AI + 23.09	Deliormanli (2012)	15 marbles
Abrasion value (AV/AVS) (mg)	Positive linear correlation	Dahl et al. (2012)	60 samples among 16 rock types
LCPC abrasivity coefficient (LAC) (g/t)	LAC = ~ 300·CAI	Büchi et al. (1995)	47 datasets
	LAC = 273·CAI	Thuro and Käsling (2009)	74 datasets
	LAC = 364.26•CAI + 605.87	Cheshomi and Moradhaseli (2017)	All 3 rock types
	LAC = 562.37•CAI – 410.33		6 granites
	LAC = 511.92•CAI + 330.59		6 gabbros
	LAC = 426.42•CAI + 493.63		6 hornfels
Rock abrasivity index (RAI = UCS·EQC) (–)	Polynomial correlation	Plinninger (2002)	60 datasets
	$CAI = 0.9 \bullet \sqrt[3]{RAI}$	Schumacher (2004)	–
	CAI = (0.53–0.91)•lnRAI + (– 0.12–0.49)	Majeed and Abu Bakar (2015)	40 samples
Schimazek wear index (F-index = 10•C_{Qtz}•d_{Qtz}•BTS) (N/mm)	$CAI = (2.17–2.77) \bullet F\text{-index}^{(0.24–0.31)}$		

coefficient (LAC) (NF P18-579 1990), Böhme abrasion (BA) and wide wheel abrasion (WWA) (EN 14157 2017). Additionally, the Schimazek wear index (F-index) (Schimazek and Knatz 1970, 1976) and the rock abrasivity index (RAI) (Plinninger 2002) serve as complex indices calculated from basic rock physical-mechanical parameters. While direct correlations between rock abrasiveness assessed by different methods reveal the versatility of measuring this property, a consistent theme emerges: rock abrasiveness can be determined in different ways. Notably, direct correlations with CAI have been identified for AV/AVS, LAC, BA and WWA (Büchi et al. 1995; Thuro and Käsling 2009; Dahl et al. 2012; Deliormanli 2012; Cheshomi and Moradhaseli 2017; Teymen 2020). Considering that rock abrasiveness contributes to tool wear, as expressed by the complex geotechnical index, i.e., RAI, it seems as a more robust index regarding rock abrasiveness. RAI captures two most dominant parameters: (1) The content of abrasive minerals within the rock relevant to tool wear; (2) The rock strength significant for both abrasive wear and tool impact failure. Bivariate correlations have been established between CAI and RAI (Plinninger et al. 2004; Schumacher 2004; Majeed and Abu Bakar 2015). Furthermore, F-index has also been correlated with CAI in either simple or multiple analyses (Majeed and Abu Bakar 2015; Ko et al. 2016).

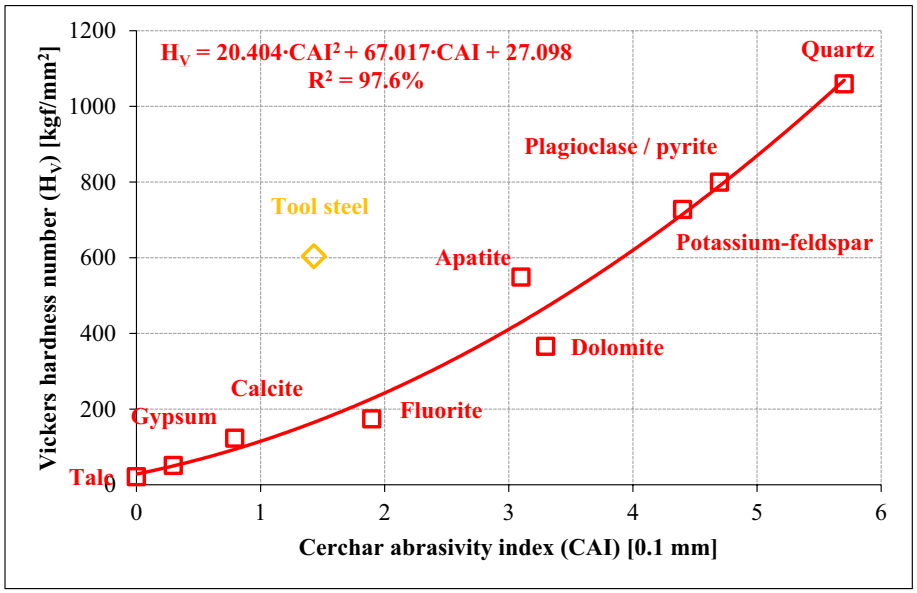

Fig. 24 Correlations between CAI and H_V (Kaspar et al. 2023, modified)

Table 10 Summary of rock brittleness and toughness influencing CAI (bivariate)

Parameters	Models	References	Remarks
Brittleness index $\left(B_1 = \frac{UCS}{BTS}\right)$ (–)	No correlation	Altindag et al. (2010)	95 datasets from literatures
Brittleness index $\left(B_2 = \frac{UCS-BTS}{UCS+BTS}\right)$ (–)	No correlation		
Brittleness index $\left(B_3 = \sqrt{\frac{UCS \cdot BTS}{2}}\right)$ (–)	$CAI = 0.104 \bullet B_3 + 0.257$		
Brittleness index $\left(B_4 = \frac{UCS \cdot BTS}{2}\right)$ (–)	$CAI = 0.0005 \bullet B_4 + 2.368$	Ündül and Er (2017)	23 andesites and rhyodacites
Mode-I fracture toughness K_{IC} (MPa $m^{1/2}$)	$K_{IC} = 0.38 \bullet CAI^{1.24}$	Teymen (2020)	80 samples
Block punch penetration index (PPI) (MPa)	$PPI = 6.59 \bullet CAI - 2.54$		
Rate of penetration $\left(ROP = \frac{\text{Depth of borehole [mm]}}{\text{drilling tims [s]}}\right)$ [mm/s]	$ROP = 57.12 \bullet CAI^{-2.49}$		
Sievers' J-value (SJ) (mm/10)	Negative correlation	Dahl et al. (2012)	66 samples among 20 rock CAI types
	$CAI = -0.424 \bullet \ln SJ + 2.96$	Yasar et al. (2015)	7 rock types
Drilling rate index (DRI related to S_{20} and SJ) (–)	$CAI = -2.092 \bullet \ln DRI + 9.83$		
Cutter life index $\left(CLI = 13.84 \cdot \left(\frac{SJ}{AVS}\right)^{0.3847}\right)$ (mm/mg)	$CLI = -8.725 \bullet \ln CAI + 18.898$	Ko et al. (2016)	38 datasets fromliteratures

4.5 Rock brittleness and toughness

Table 10 summarizes the rock brittleness and toughness influencing CAI. Brittleness, a fundamental characteristic of rocks, plays a pivotal role in the fragmentation process and the excavatability of rocks (Hucka and Das 1974; Wilfing 2016). This property can be evaluated based on rock strength attributes, with the UCS-to-BTS ratio emerging as a reliable indicator of brittleness. This ratio effectively characterizes rock's resistance to cutting or drilling, as it considers compressive strength relevant to rock indentation and crushed zone formation, as well as tensile cracks crucial for the generation of rock chips. Seen from Table 10, four distinct brittleness indexes (B_1-B_4) have been developed in relation to CAI, with B_3 demonstrating the strongest correlation, except for metamorphic rocks (Altindag et al. 2010). However, establishing straightforward regression models for CAI based on brittleness indexes of B_1, B_2 and B_3 has proven elusive. Ko et al. (2016) found that combining

brittleness indexes with UCS or BTS, or both, enhances the prediction of rock abrasiveness. Furthermore, Ündül and Er (2017) determined that, among the three brittleness indexes (B_1, B_2, and B_4), only B_4 exhibits an acceptable connection with CAI. Another approach to determine rock brittleness involves laboratory tests, categorized as impact and rotary tests. In impact tests, parameters like the brittleness value (S_{20}) (Matern and Hjelmer 1943) and the punch penetration index (PPI) (Yagiz 2009) are used to gauge a rock's resistance to crush under repeated impacts. These parameters illuminate the rock behaviour when subjected to impactor's indentation. Meanwhile, rotary tests, exemplified by Sievers' J-value (SJ) miniature test (Sievers 1950) and other caliber core drilling tests using rate of penetration (ROP), reveal the rock failure characteristics. Derived from three fundamental parameters, AV/AVS, S_{20} and *SJ*, as proposed by NTNU (Bruland 1998), three complex parameters capture cutting or drilling efficiency and tool lifetime: (1) The drilling rate index (DRI), factoring in the rock's ability to withstand repeated impacts (S_{20}) corrected by its surface hardness (SJ), provides an insight into dill bit lifetime; (2) The bit wear index (BWI), calculated from DRI and AV, estimates the drill bit lifetime; (3) The cutter life index (CLI), derived from SJ and AVS, predicts the TBM disc lifetime. Dahl et al. (2012) established correlations between SJ (ranging from extremely high to extremely low surface hardness, 1.6–95.5) and CAI (ranging from medium abrasive to quartzitic, 1.5–6.9). Additionally, DRI and CLI have also related to CAI through various correlations (Yasar et al. 2015; Majeed and Abu Bakar 2015; Ko et al. 2016).

Rock toughness, defined as the resistance to crack propagation, is another aspect indicative of a rock's resistance, particularly during the cutting process. Predicting rock abrasiveness has involved considering fracture toughness. According to the Irwin fracture criterion (Irwin 1958), the Cerchar scratching process appears to represent the mode-II fracture toughness, but laboratory tests conducted by Alber (2008) and Teymen (2020) primarily aim to determine the mode-I fracture toughness. Alber (2008) selected chevron bend samples (ISRM 1988) and found no obvious correlation, while Teymen (2020) tested semi-circular bend samples (Chong and Kuruppu 1984) and established a power one.

5 Applications of Cerchar test in material science, tribology and rock engineering

5.1 Investigation of tool wear

In material science, with the aid of the Cerchar test, Küpferle et al. (2015) delved into the abrasive characteristics of various steel materials, including construction steel, quenched and tempered steel and tool steel (i.e., cemented carbide). Experimental findings demonstrated that ferritic materials displayed the highest abrasive tendency due to their low hardness, martensitic materials ranked next in terms of abrasive behaviour, and carbide-rich materials exhibited the lowest abrasive tendency. This underscores the superior wear resistance of carbide-rich steels against rock's abrasiveness. Piazzetta et al. (2018) conducted an analysis of wear behaviour observed on the stylus tip and related it to groove mechanisms. Their investigation categorized abrasive wear into three distinct regimes based on the observed conditions of abraded tip surface. These regimes were then linked to the corresponding CAI values for the tested rocks. Figure 25 provides insights into the primary tip wear mechanisms observed through scanning electron microscope (SEM) after scratching different types of rocks. Notably, abrasive quartzites (CAI = 5.5) exhibited severe wear characterized by micro-cutting and extensive plastic deformation of the stylus, as shown in Figs. 25g–i. Transitional wear surface, marked by micro-fatigue, were observed when scratching basalt (CAI = 1.0) and syenogranite (CAI = 1.8 and 3.1), as illustrated in Figs. 25c–f. Mild wear, manifesting as a polished stylus surface, was evident in marble (CAI = 0.3), as shown in Fig. 25b. In essence, abrasive wear is predominantly resulted from grooving and micro-cracking. In most cases, abraded steel surfaces exhibit characteristic signs of severe plastic deformation due to scratching on hard and abrasive minerals, enduring high contact stress. This abrasive wear leads to the removal of steel material through cracking, chipping, delamination, dislocation and displacement of steels. Typical wear phenomena include narrow or wide, shallow or deep grooves with or without rock debris, and a regular or chaotic alignment relative to the scratching direction of the stylus (Münch et al. 2023; Zhang et al. 2024).

In tribology, the Cerchar scratching process can be likened to two-body abrasion between rock and stylus. However, it is important to note that three-body abrasion may also occur when encrusted hard minerals on the tip advance alongside the stylus (Burwell 1957; Moore 1974; Moore and King 1980; Zum Gahr 1987). It is worth emphasizing that the actual scratching scenario within a tribosystem is complex and may involve a combination of various wear mechanisms simultaneously. Identifying tool wear mechanisms during the scratching of different rocks holds significant value for cutter head design (i.e., size, shape, and geometry), tool material selection (i.e., metallurgy and hardness) and tool lifetime prediction (i.e., wear rate).

5.2 Failure mechanism of rock scratching or cutting

The failure mechanism of rocks induced by indenting or cutting tools can be classified as either ductile or brittle. Ductile behaviour leads to the development of a damage zone, while brittle behaviour involves the growth of macro-cracks

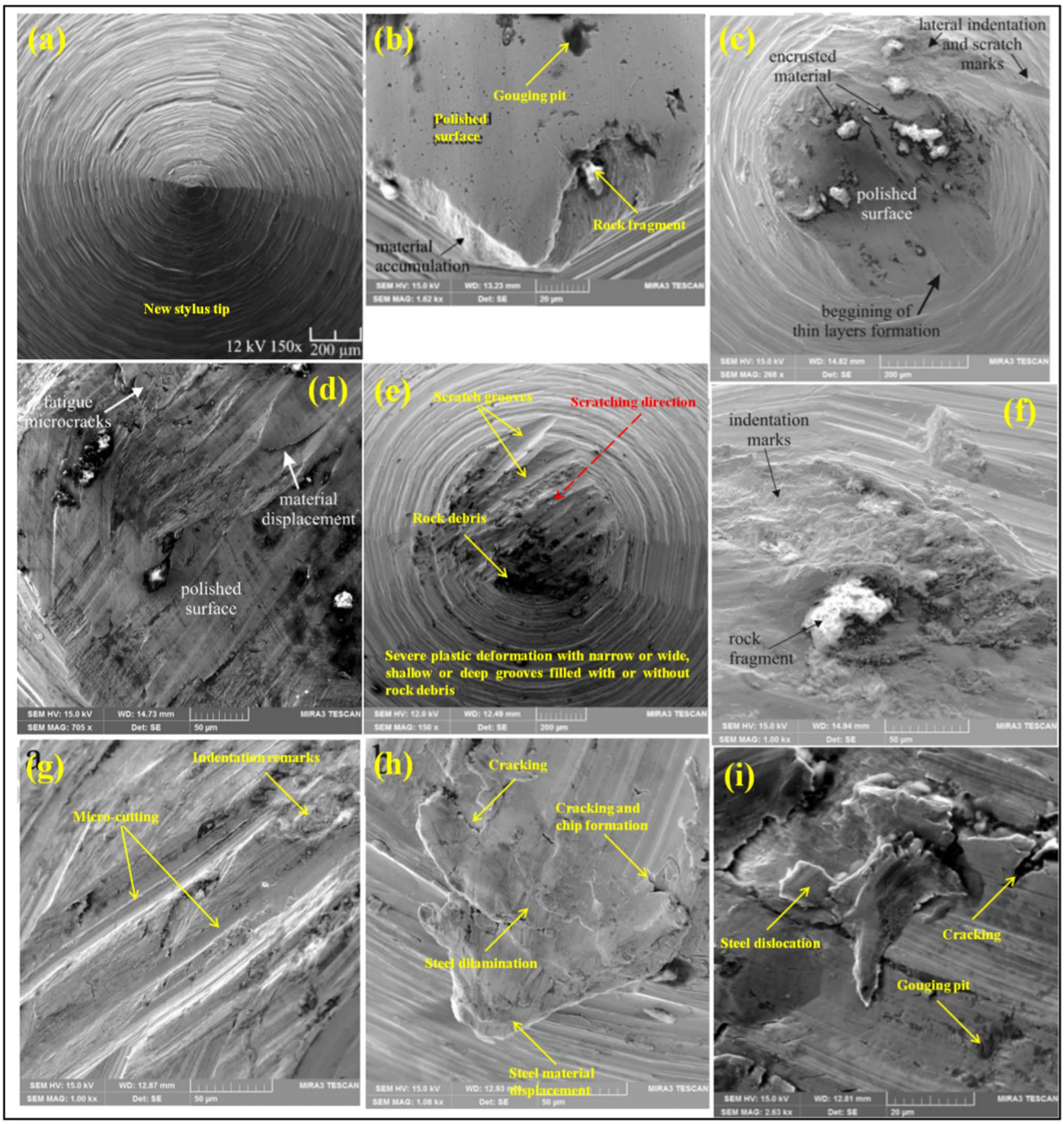

Fig. 25 SEM observation of abrasive wear on the abraded stylus tip after rock scratching: **a** New stylus; **b** Marble (CAI = 0.3); **c** Basalt (CAI = 1.0); **d** Syenogranite (CAI = 1.8); **e**, **f** Syenogranite (CAI = 3.1); **g**–**i** Quartzite (CAI = 5.5) (Piazzetta et al. 2018, modified)

(Huang and Detournay 2012; Huang et al. 2013), as shown in Fig. 26. Analyzing the scratch grooves on rock surface can provide insights into its fracture behaviour when subject to indenting and/or cutting.

Wang and Clausen (2002) performed an indenting-cutting test on marble by using a single point cutting tool, and concluded that plastic deformation and fracture chipping of material are the dominant damage and material removal processes. Hamzaban et al. (2014) investigated scratch grooves on various types of rocks, ranging from non-abrasive to extremely abrasive, and discussed groove shapes in relation to their abrasive classifications, as shown in Fig. 27. Meanwhile, SEM examinations of scratch grooves conducted by Zhang and Konietzky (2020) provided a deeper

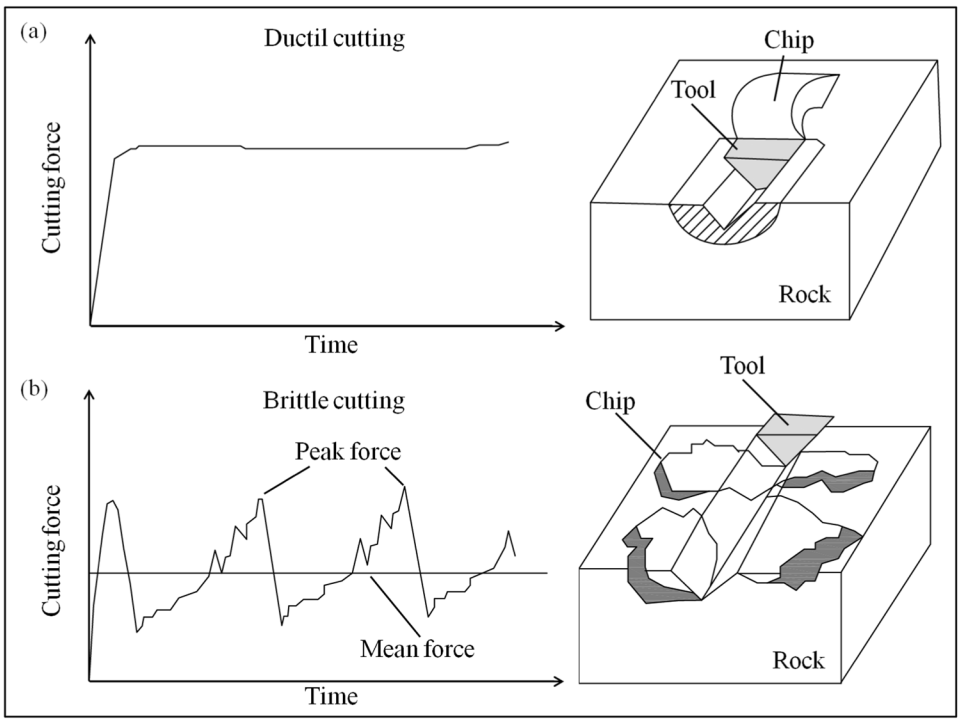

Fig. 26 Failure modes of rock cutting: **a** Ductil cutting; **b** Brittle cutting (Zum Gahr 1987, modified)

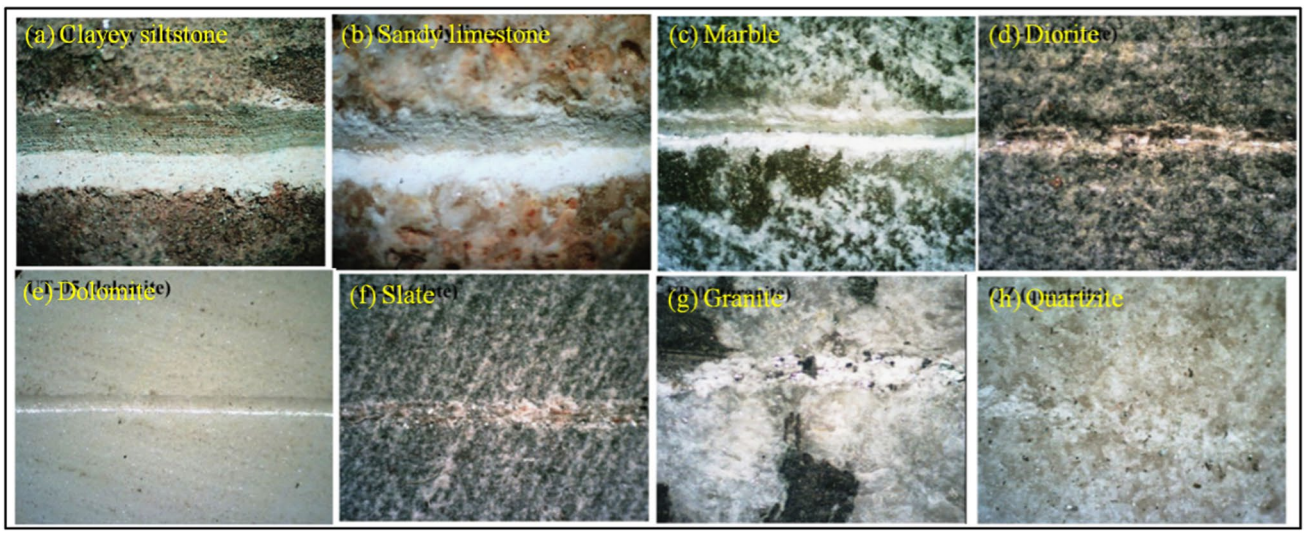

Fig. 27 Scratch pictures of surface grooves for **a** Siltstone (CAI = 0.2); **b** Limestone (CAI = 0.8); **c** Marble (CAI = 1.06); **d** Diorite (CAI = 2.07); **e** Dolomite (CAI = 0.89); **f** Slate (CAI = 2.43); **g** Granite (CAI = 4.13); **h** Quartzite (CAI = 3.88) (Hamzaban et al. 2014, modified)

understanding of fracturing on damaged rock surfaces. In most cases, mineral grains detach from the damaged surface through fracturing after plastic deformation on the stressed surface, as shown in Fig. 28. The transition from plastic deformation-induced wear to cracking-induced wear can be attributed to the rock fabric characteristics, such as pore structure, grain size, mineral composition and especially the presence of hard and abrasive minerals. Figure 29 depicts the groundmass of the rock surface scratched by the stylus, revealing that altered or opacified minerals allow for wider scratches (resulting in less tip wear), while groundmass composed of quartz and orthoclase leads to narrow scratches that retain more stylus remnants (resulting in more tip wear) (Ündül and Er 2017). In addition, Perez et al. (2015) delved into how rock fracturing evolves under the cutting action. They used acoustic emission (AE) sensors on both the

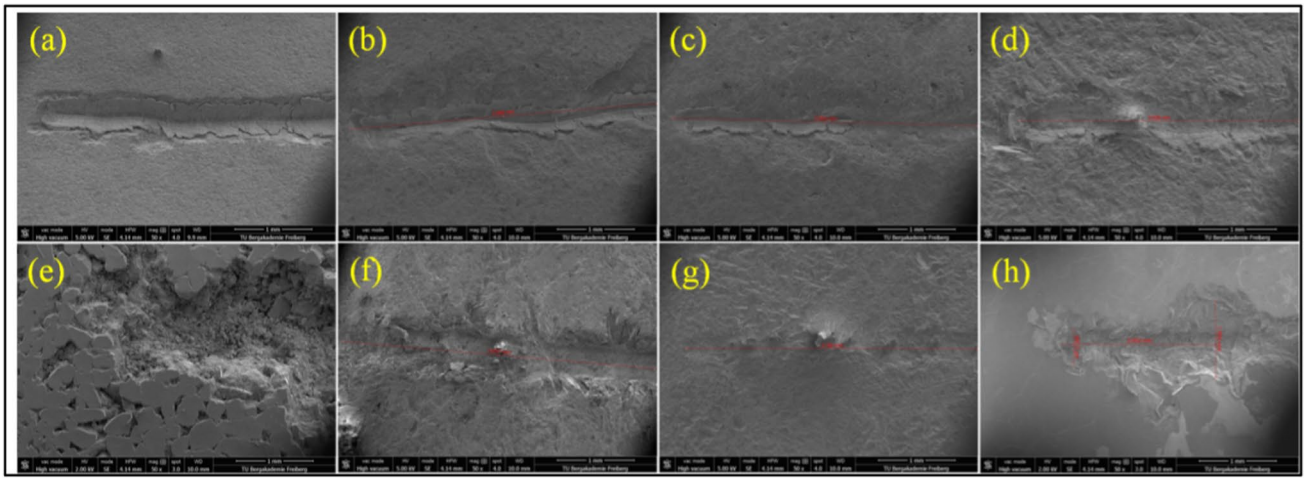

Fig. 28 SEM micrographs of scratch grooves on **a** Slate (CAI = 0.79); **b** Dolomite (CAI = 1.54); **c** Limestone (CAI = 1.65); **d** Greywacke (CAI = 2.71); **e** Sandstone (CAI = 2.50); **f** Gneiss (CAI = 3.84); **g** Diorite (CAI = 3.58); **h** Granite (CAI = 4.10) (Zhang et al. 2020a, modified)

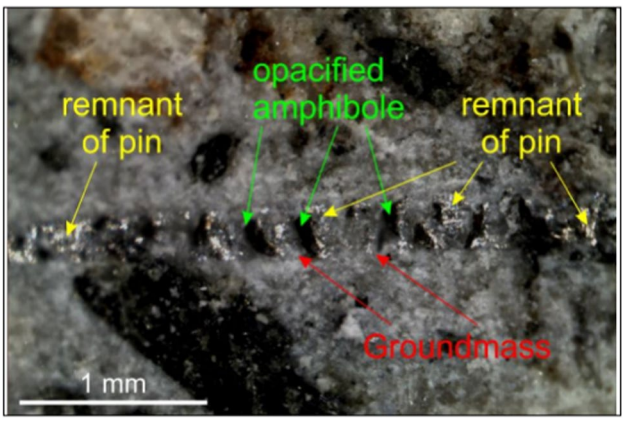

Fig. 29 Observation on scratch of the stylus over the rock surface (Ündül and Er 2017)

tested rock and testing apparatus, establishing a correlation between CAI and the total numbers of events.

Regarding the Cerchar scratching mechanism, Suana and Peters (1982) emphasized the significant role of rock texture, including grain size, composition and content and mineral hardness, in influencing stylus movement and resultant CAI. In the case of low-strength sandstone, the stylus continuously penetrates the rock during scratching, resulting in wear predominantly on the side of the stylus, rather than on its tip, and leading to an underestimation of CAI. Al-Ameen and Waller (1994) examined the Cerchar mechanism considering hard and soft rocks with respect to their strength properties. They noted that at the start of scratching process, the stylus penetrates the rock due to high pressure on its tip. The maximum penetration depth is reached when equilibrium is achieved between the stress applied to the stylus and rock strength. For hard rocks, the stylus cannot further indent the rock beyond this point and tends to move toward the sample surface due to high rock strength. Conversely, for soft rocks, the stylus continues to indent the rock due to its relatively low strength. In this scenario, CAI is dependent on the rock texture. Rocks devoid of hard and abrasive minerals exhibit no increase in tip wear with sliding distance, while rocks containing abrasive minerals resulting in continuous stylus tip wear until the end of testing. These findings were confirmed by Zhang et al. (2020b), who identified three stylus movement regimes, as shown in Fig. 30. The authors concluded that the fluctuation in penetration depth can be attributed to rock heterogeneity and microstructure. Notably, the significant fluctuation of depth in sandstone is not attributed to the measurement errors but linked to the pore structure of this rock. Penetration depth stands out as the most influential factor affecting scratching force. This phenomenon is supported by the higher scratching force required for sandstone due to its greater penetration depth, compared to slate and granite.

5.3 Numerical modeling of combined rock indenting and cutting

Rock cutting processes, which are essential in various operational conditions, have been extensively modeled to detect crack formations beneath the rock surface using the discrete element method (DEM). Some notable works include Su and Akcin (2011), Rojek et al. (2011), Huang et al. (2013), Van Wyk et al. (2014) and Zhang et al. (2020d). However, there has been relatively limited focused on replicating the Cerchar scratching process, particularly in terms of addressing tip wear resulting from rock-tool interactions and detecting crack initiation and propagation during rock indenting and simultaneous cutting. It is important to note that unlike

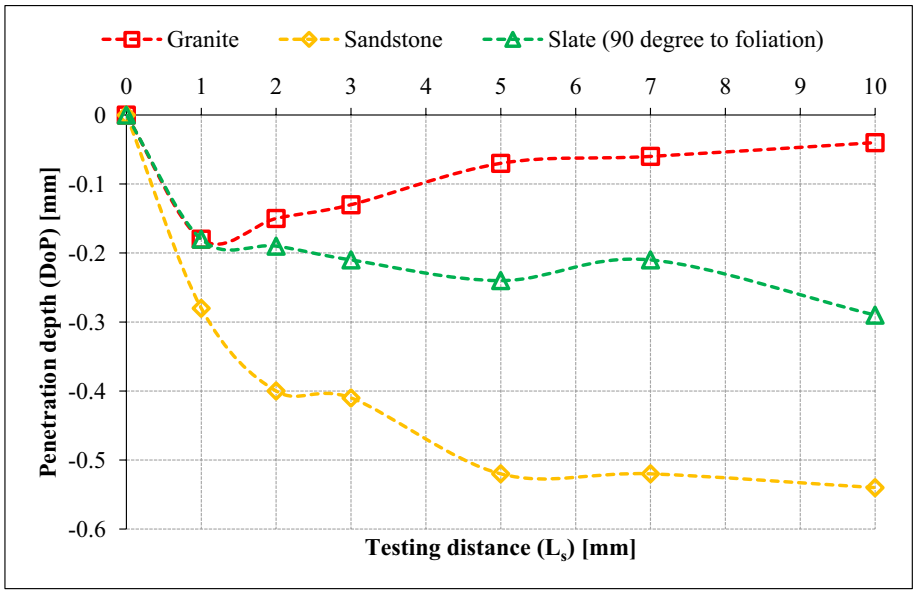

Fig. 30 Evolution of penetration depth for granite, sandstone and slate, respectively (Zhang 2020, modified)

rock cutting, where the depth of cut remains fixed during the process, the Cerchar scratching process involves the stylus penetration into the rock as it scratches the surface.

Balani et al. (2017) used the particle flow code of PFC^{3D} (Itasca 1999) to explore the effects of stylus hardness, sliding distance, scratching velocity and applied load on wear formation on the stylus tip, which consists of a particle assembly and can be wear down during scratching. The simulations results closely mirrored the experimental results, highlighting the accuracy of the model. Recently, Zhang et al. (2022a) developed a model for the Cerchar scratching process that incorporates a servo-mechanism to mimic the actual stylus action (Itasca 2014). As illustrated in Fig. 31a, the monitored scratching force- and depth-displacement curves closely resemble the experimental results, reaffirming the fidelity of the DEM model in representing the combined rock indenting and cutting process. Notably, numerical modeling indicates that the number of tensile cracks is approximately three times higher than those of shear cracks, underscoring the dominance of tensile failure in rock scratching and cutting, as shown in Fig. 31b.

5.4 Estimation of rock-stylus interaction, tool performance and rock excavatability

In rock engineering, gaining a comprehensive understanding of the interaction between rock and tools holds immense significance. This knowledge can greatly enhance rock-breaking performance and enable the optimization of cutting or drilling parameters. However, performing real and large-scaled cutting or drilling experiments can be prohibitively expensive. To address this challenge, the Cerchar test, considered as a model-test, offers a valuable alternative. It allows for the investigation of rock-stylus interaction, the evaluation of tool performance and the estimation of rock excavatability.

Hamzaban et al. (2014) and Hamzaban et al. (2018) introduced two novel performance parameters. The first, known as the modified Cerchar abrasivity index (MCAI), relates CAI to horizontal force. Experimental findings demonstrated that MCAI exhibits stronger associations with rock mechanical properties than CAI, making it a more promising indicator for estimating tool wear. The second parameter considers the energy consumed during rock scratching, akin to the concept of specific energy in the rock cutting — an important parameter in rock engineering for evaluating cutting efficiency. The parameter, referred to as the scratch energy index (SE$_i$), demonstrates reasonable correlations with rock hardness and mechanical properties. It enables the comparison of tool performance across different hardness levels when producing scratches on various types of rocks, as shown in Fig. 32. In an innovative contribution, Zhang and Konietzky (2020) introduced the Cerchar abrasion ratio (CAR), calculated as the ratio of material volume removed from the rock surface to the wear volume abraded on the stylus tip. Notably, CAR exhibits an inverse correlation with CAI, suggesting that as rock abrasiveness decreases, cutting effectivity increases, as shown in Fig. 33a. Unlike CAI, which is solely based on the abraded tip, CAR takes both rock and tool into account, providing a more comprehensive evaluation of rock cutting effectivity. This makes CAR a meaningful parameter for designing and making decision regarding rock cutting process. Furthermore, Zhang et al. (2020a, b) investigated the energy consumed during rock scratching and introduced a parameter known as Cerchar specific energy (CSE). CSE serves as an additional descriptor of

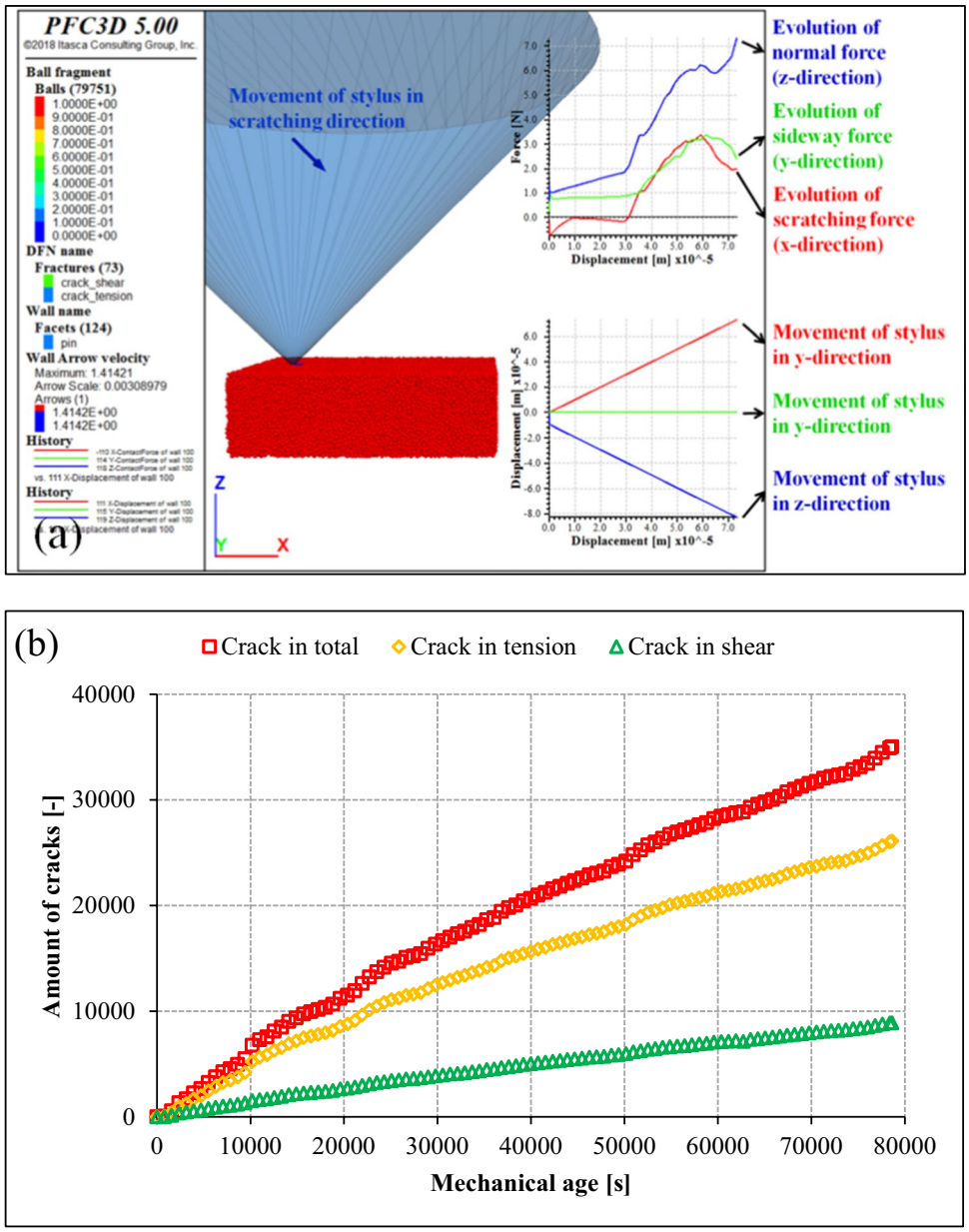

Fig. 31 Evolution of **a** Normal, scratching and sideway forces; **b** Numbers of cracks with stylus movement by using PFC^{3D} (Zhang et al. 2022a, modified)

the rock-stylus interaction and cutting efficiency. Experimental results showed an exponential correlation between CSE and CAI, as shown in Fig. 33b, making it a valuable tool for assessing rock abrasiveness. As a pioneer work, Rossi et al. (2018) and Rossi et al. (2020) compared tool performance by conducting the Cerchar tests on granite and sandstone samples before and after subjecting them to heat treatment at 800 °C. They introduced a drillability index, calculated as the ratio of scratching force to penetration depth. As shown in Fig. 34, the slopes of the fitted lines indicate that the drillability index decreases after heat treatment. This reflects the enhanced drilling efficiency of thermally treated rock materials, achieved by increasing the penetration depth and reducing the cutting forces.

5.5 Prediction of tool lifetime

Another main application of CAI in rock engineering is to predict the lifetime of mechanical tools. High rock abrasiveness is known to accelerate tool wear (Deketh 1995; Verhoef 1997; Frenzel et al. 2008; Farrokh and Kim 2018; Capik and Yilmaz 2021). Over time, scholars have established correlations or empirical formulas relating tool lifetime to CAI, UCS, or their combination of rocks.

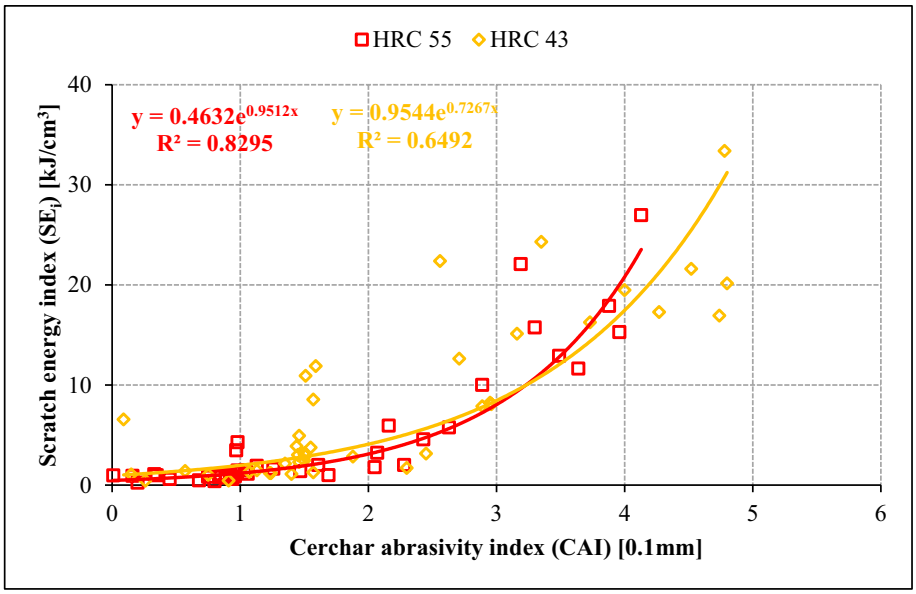

Fig. 32 Correlations between SE_i and CAI (Hamzaban et al. 2018, modified)

For drag picks, several studies have established linear correlations between pick consumption and CAI for coal sedimentary rocks (Nizamoglu 1978; Johnson and Fowell 1986; Bilgin 1989; Yarali et al. 2008). For conical picks, the Austria Voestalpine Ltd. developed a model linking conical pick consumption to both UCS and CAI for rocks characterized by lower strength and low to medium-high abrasiveness (Plinninger et al. 2004). Based on the trans-Alpine Mont Cenis tunnel project, the Sweden Sandvik Group established a correlation between the consumption of a 22 mm diameter pick and the combined UCS and CAI for the tunnel miner MT620 (Restner and Pichler 2007). For drill bits, a weak linear correlation was found between the consumption of a 45 mm diameter drill bit and CAI (Plinninger et al. 2004). For disc cutters, Büchi (1984) introduced a pivotal approach to determine the wear rate of a mini disc cutter, which is roughly one-tenth the size of a standard cutter. The wear rate of these mini discs, named the Mini Disc Wear Rate (MDWR), quantifies the mass of steel worn off the disc per unit volume of rock extracted from the core. Notably, MDWR exhibits a quadratic correlation with CAI, unveiling a valuable correlation. Wijk (1992) introduced a theoretical model for predicting the rolling length of a wedge-shaped disc cutter. This model takes critical factors into account, such as the applied thrust force, the tool geometrical parameters including disc diameter and edge angle, as well as the intrinsic rock parameters like UCS and CAI. Expanding on the idea that cutter wear may be linked to CAI, Gehring (1995) established a power correlation, further enhancing our understanding of the correlation between CAI and tool performance. Rostami et al. (2005) formulated a predictive equation for estimating the lifetime of a 17-inch disc cutter. Their findings revealed an inverse correlation between the cutter lifetime and CAI, shedding light on the critical role of CAI in cutter durability assessments. Maidl et al. (2001) conducted research to correlate the wear rate of a 17-inch disc cutter with a combination UCS and CAI, offering a comprehensive perspective on the multifaceted factors influencing cutter wear. Drawing from several tunnel projects, Bieniawski et al. (2009) established an evaluation framework that hinges on the rock mass excavatability (RME) index, rock compressive strength and Cercahr abrasivity for predicting the cutter consumption, defined as the amount of cutter wear per unit of excavated rock. The RME, a rating value, is closely linked to the prevailing geological conditions. In a similar vein, Liu et al. (2017) developed empirical correlations between the wear rate of a 20-inch disc cutter and rock intrinsic properties, among which two rock properties, CAI and UCS, demonstrated strong correlation with the average cutter lifetime (E_f). Table 11 provides an overview of prediction models for calculating tool consumption or lifetime by means of CAI. Overall, different models give a wide range of variation for lifetime prediction. Particularly for disc cutters, CAI is the key parameter in the models of Gehring (1995), Maidl et al. (2001) and CSM (Rostami et al. 2005). It is important to note that the Gehring model relies on a real tunnel project and considers the TBM parameters, including disc position, cutter ring loss and penetration rate, but the selected datasets were relatively rare. Moreover, RME (Bieniawski et al. 2009) and E_f (Liu et al. 2017) consider the CAI value as a control value for chart estimation.

5.6 Sensitivity of rock abrasiveness to high stress and temperature

Alber (2008) raised a pertinent concern regarding potential underestimation of rock abrasiveness when subjected to high in-situ stress conditions. To address this issue, the author

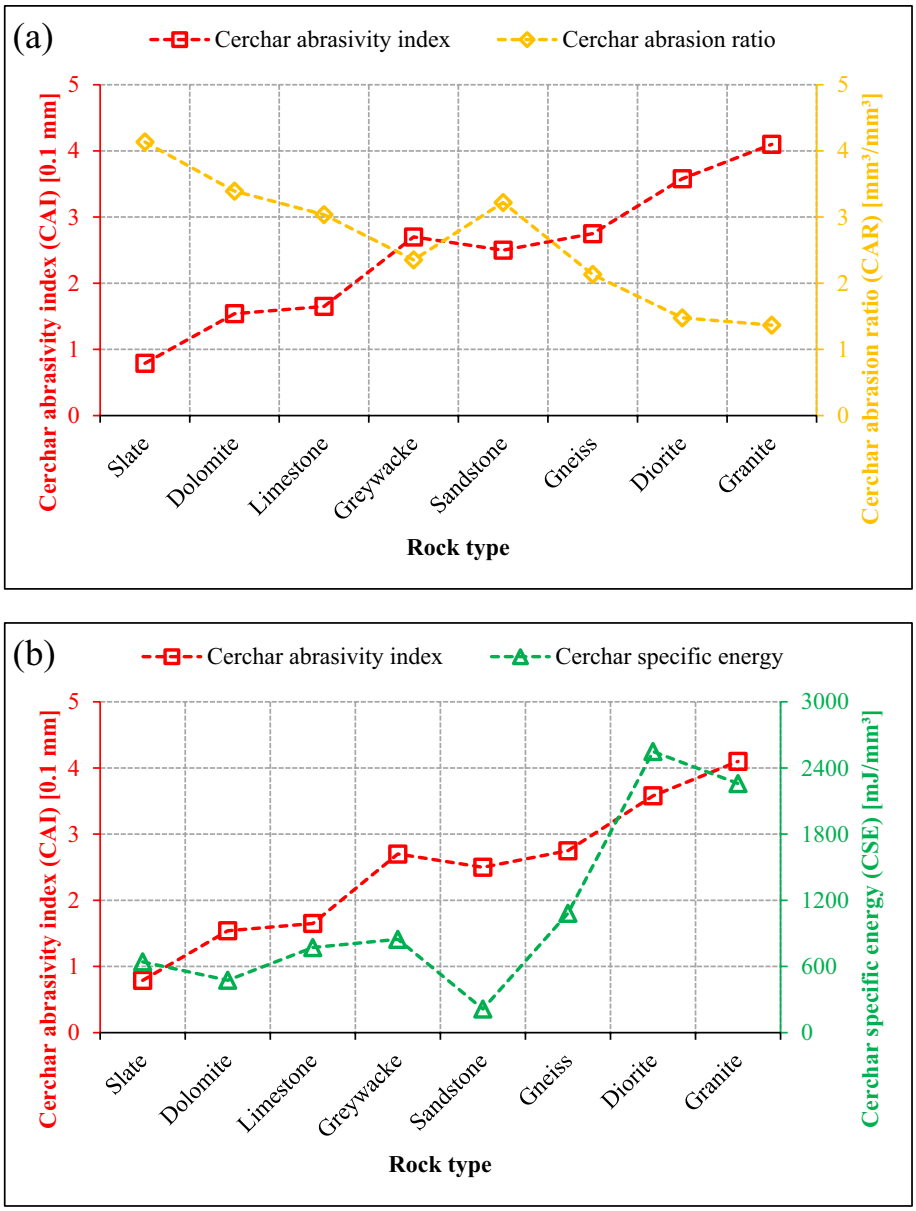

Fig. 33 Evolutions of **a** CAR and CAI; **b** CSE and CAI (under sawn surface condition) (Zhang and Konietzky 2020; Zhang et al. 2020a, modified)

conducted a comprehensive set of Cerchar tests using Hoek's cell. Experimental results revealed a noteworthy disparity in CAI values when lateral confinement is applied, showing higher values compared to tests conducted without it. Eberl et al. (2008) explored the influence of temperature on rock abrasiveness, aiming to see if the transformation of quartz mineral from low to high temperature influencing rock abrasiveness. Results showed that CAI decreases, as temperature rises for both granite and sandstone. These findings were confirmed by Rossi et al. (2018). However, Ji et al. (2020) found that CAI value initially drops with increasing temperature up to 600 °C when testing granite sample. Beyond 600 °C, it begins to rise, peaking at 800 °C. More recently, Wang et al. (2023) studied the effect of cooling rate (slow vs. rapid cooling) on rock abrasiveness, brittleness, crack formation and penetration stress. Their findings indicated that slower cooling leads to increased rock brittleness and higher indentation stress, making it less accommodating for stylus penetration. Abu Bakar et al. (2023) studied the combined effect of temperature and confining pressure on rock abrasiveness. After heat treatment, two types of granite samples were tested under different lateral confinements using Hoek's cell. Experimental results showed that, for both granites, the CAI values decrease with increasing temperature from 25 °C to 500 °C at all confinement conditions, but at 600 °C, the CAI values become nearly equal to those at ambient temperature of 25 °C. Moreover, a linear increase in CAI with increasing confining pressure was observed for all treatment temperatures. After testing six different rock materials, Zhang et al. (2024) concluded that quartz-rich

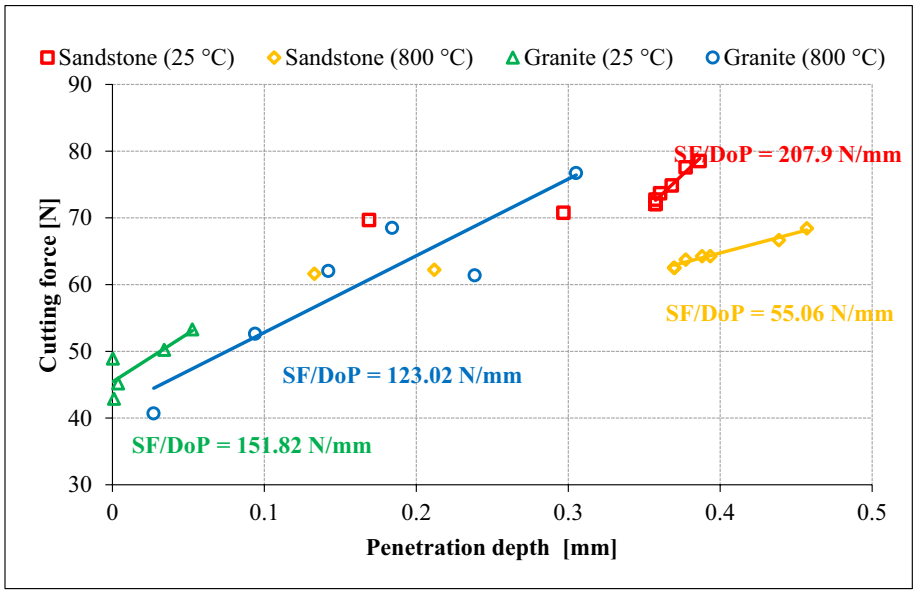

Fig. 34 Evolutions of scratching force with penetration depth for sandstone and granite at 25 °C and 800 °C, respectively (Rossi et al. 2018; Rossi et al. 2020, modified)

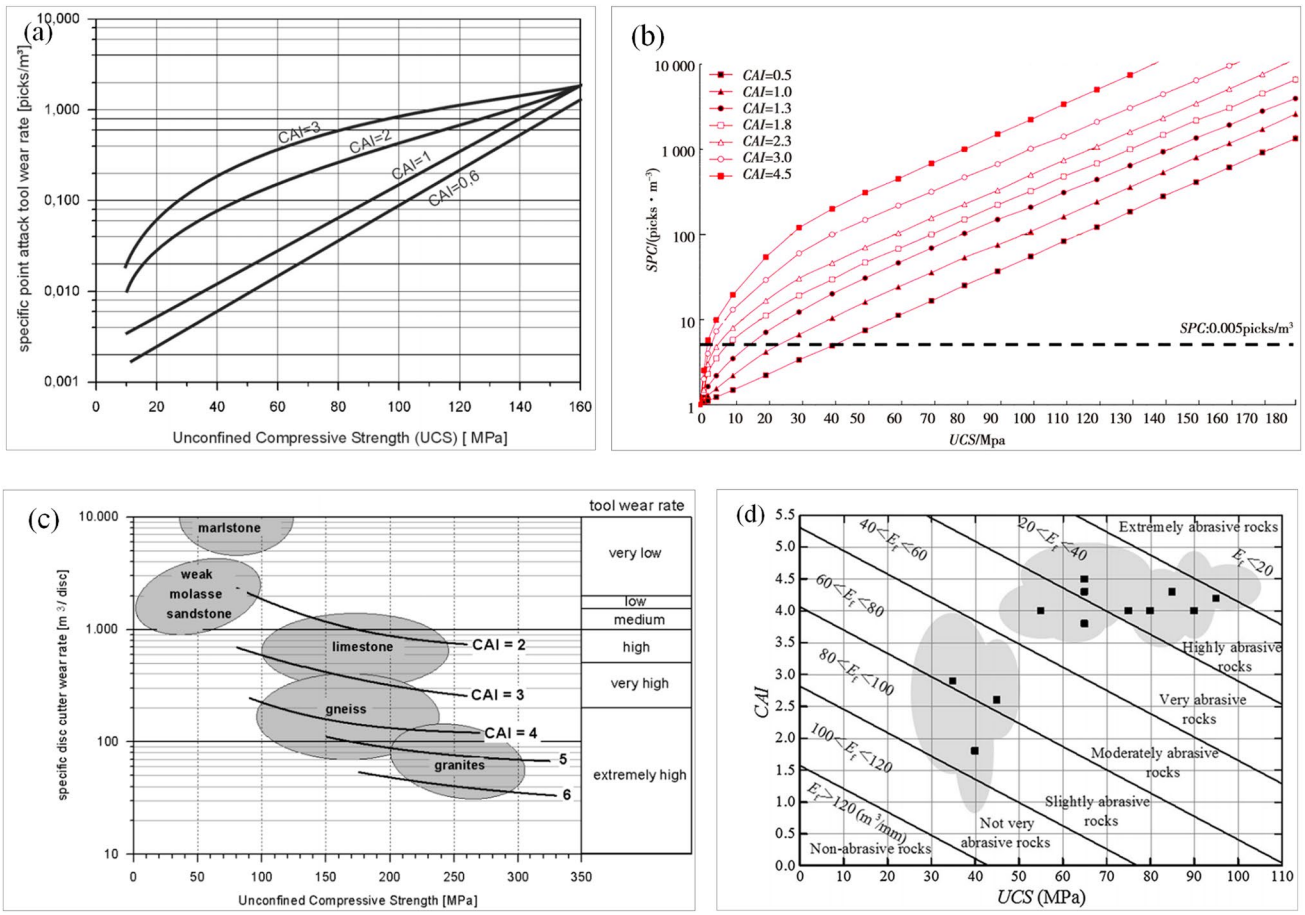

Fig. 35 Wear prediction of mechanical tools using CAI or CAI-UCS (Chart estimation) (**a** Plinninger et al. 2004; **b** Restner and Pichler 2007; **c** Maidl et al. 2001; **d** Liu et al. 2017, modified)

Table 11 Wear prediction models for mechanical tools utilizing CAI

Parameters	Calculation models	References	Remarks
Drag picks			
Tool consumption (tools/m^3)	$TC = 0.2228 \bullet CAI + 0.0258$	Nizamoglu (1978); Johnson and Fowell (1986); Bilgin (1989)	Drag pick; Coal sediments
	$TC = 0.2533 \bullet CAI - 0.0948$	Yarali et al. (2008)	
Roadheader picks			
Tool consumption (bits/t)	$TC = \frac{CAI}{4} \bullet k_1 \bullet k_2$	Rostami et al. (2005)	Tool consumption of a medium to heavy duty roadheader; $k_1 = 0.75–1$ for cutterheads with water jet spray and effectiveness of the jets; $k_2 = 0.9–1.2$ is a constant related to cutterhead velocity
Specific pick wear rate (picks/m^3)	Wear rate is related to combination of CAI-UCS	Austria Voestalpine Ltd. (in Plinninger et al. 2004)	Conical pick; for rocks with relatively low strength and abrasivity; Chart estimation (see Fig. 35a)
Specific pick consumption (picks/m^3)	Pick consumption is related to combination of CAI-UCS	Restner and Pichler (2007)	22 mm diameter pick; Chart estimation (see Fig. 35b)
Cutter consumption rate (cutters/m^3)	$CCR = 0.0745 \bullet CAICAI - 0.0364$	Comakli (2019)	Conical pick; 75 t weight roadheader
Drill bits			
Drill bit life (m/bit)	Negative linear correlation	Plinninger et al. (2004)	45 mm diameter drill bit; 15 datasets; $R^2 = 0.26$
Bit working life (m/bit)	$BL = -2049 \bullet \ln CAI + 3398.1$	Majeed et al. (2019)	BL = Bore holes drilled per day x depth of each bore hole x drill bit replacement times (m/bit); In-situ drill test in Pakistan
TBM discs			
Mini disc wear rate (g/m^3)	$MDWR = 1.1 \bullet CAI^2$	Büchi (1984)	MDWR = Mini disc wear rate (Mass of steel worn off the disc per volume of rock cut from the core) (g/m^3); 1/10 of real cutter; 15 rocks; laboratory test
Cutter life (m)	$L = \frac{\sum Dw^3 \cot\theta}{F\sqrt{\sigma_c \sigma_{PLT}} CAI^2}$ $w = 2\rho\sqrt{1 - \left(\frac{\pi}{2} - \theta\right)\tan\theta}$	Wijk (1992)	L = Cutter life (Rolling length of disc cutter) (m); D = Diameter of disc cutter [m]; w = Wear flat of disc cutter [m]; 2θ = Wedge-shaped edge angle of disc cutter [°]; F_T = Thrust force [N]; σ_c = Uniaxial compressive strength of rock [Pa]; σ_{PLT} = Point load index of rock [Pa]; Theoretical model
Specific weight loss (mg/m)	$W_f = 0.74 \bullet CAI^{1.93}$ $W_f = \frac{8 \bullet \pi \bullet D \bullet T \bullet TL}{S_r}$	Gehring (1995)	W_f = Specific weight loss (Weight loss of cutter per rolled meter) [mg/m]; D = Diameter of disc cutter [m]; T = Width of cutter ring[m]; TL = Diameter reduction of disc cutter [m]; S_r = Rolling distance of the cutter [m]; Real tunnel project; Gehring model
Specific disc cutter wear rate (m^3/disc)	Wear rate is related to combination of CAI-UCS	Maidl et al. (2001)	Chart estimation (see Fig. 35c)
Cutter life (10^6 feet)	$LF = \frac{6.75D}{17CAI}$	Rostami et al. (2005)	LF = Cutter life (Linear feet of cutter travel on the face) [10^6 feet]; D = Diameter of disc cutter [feet]; *CSM* model
Cutter life (m^3/cutter)	$CL = \frac{1026}{CAI}$	Frenzel (2011)	17-inch disc cutter with 10 cm spacing on the head and 5 mm/rev penetration

Table 11 (continued)

Parameters	Calculation models	References	Remarks
Cutter consumption (cutters/m^3)	$CAI > 3.0, CC = \frac{7 \cdot 10^6}{RME^{4.8}}$ $1.5 < CAI < 3.0, CC = \frac{628}{RME^{2.77}}$ $CAI < 1.5, CC = \frac{15}{RME^{1.96}}$	Bieniawski et al. (2009)	CC = Cutter consumption (Changed cutters/excavated m^3); Compressive strength ≥ 45 MPa, CC is correlated with RME = Rock mass excavatability index; Compressive strength < 45 MPa, Chart estimation
Wear coefficient (mm/km)	$c_v = \frac{a}{S_r}$ is related to CAI	Frenzel (2011)	c_v = Wear coefficient (mm/km); a = Radial wear of the cutter [mm]; S_r = Rolling distance of the cutter [km]; Positive correlation between c_v and CAI; Chart estimation
Average cutter life (m^3/mm)	$E_f = -26.532 \cdot CAI + 145.086$ $E_f = -16.079 \cdot CAI - 0.587UCS + 145.295$ $E_f = \frac{\pi D^2 L}{4M}$	Liu et al. (2017)	E_f = Average cutter life (rock excavation volume per cutter wear extent) [m^3/mm]; D = Tunnel diameter [m]; L = Excavated tunnel length [m]; M = Total wear extent of all disc cutters used on the cutter head, including normal and abnormal wear extents [mm]; Chart estimation (see Fig. 35d)

Table 12 Researches on sensitivity of rock abrasiveness to confining pressure and temperature

References	Conclusions	Remarks
Alber (2008)	The CAI value measured with lateral confinement is higher than that without it	Sandstone; Greywacke; Granite; Schist
Eberl et al. (2008)	CAI decreases with increasing temperature until 900 °C	Sandstone; Granite
Rossi et al. (2018)	CAI values are lower at 800 °C than those at 25 °C	Sandstone; Granite
Ji et al. (2020)	CAI increases with temperature up to 600 °C, and then decreases until 800 °C	Granite
Abu Bakar et al. (2023)	CAI decreases with increasing temperature from 25 °C to 500 °C at all confinement conditions, but at 600 °C, CAI becomes nearly equal to those at 25 °C	2 granites
Zhang et al. (2024)	Rock abrasiveness is sensitive to temperature for quartz-rich rocks, and 500 °C is a critical value for the change of rock abrasiveness	Sandstone; Greywacke; Granite; Porphyry; Diorite; Gneiss

rocks exhibit temperature-sensitive abrasiveness, with 500–600 °C representing a critical threshold for changing abrasiveness. Conversely, the temperature effect on quartz-poor rocks is less pronounced. Table 12 summarizes the current researches on the sensitivity of rock abrasiveness to confinement and temperature. Overall, assessing CAI before and after heat treatments and/or without or with confining pressure offers valuable insights into resulting material abrasiveness and potential reduction in tool wear induced by high in-situ stresses and temperatures.

6 Summary and prospectives

6.1 Summary

In hard rock mining and tunneling, excavation cost primarily hinges on cutting or drilling efficiency, which, in turn, is significantly influenced by tool wear. The key factor affecting tool wear is the rock abrasiveness. To assess rock abrasiveness, to predict tool wear and to evaluate tool performance, the Cerchar test serves as a valuable model-test. Table 13 summarizes the published articles, standards and theses on the Cerchar test since its inception.

For the Cerchar test itself, to enhance the measurement accuracy of CAI, several suggestions pertaining to testing conditions are offered: (1) Use an automatic testing device to achieve better control and measurement of testing distance and velocity, instead of manual operations; (2) When dealing with soft rocks like siltstone and mudstone, consider using a relatively lower hardness number (e.g., HRC 40–42) to mitigate wear on the side of stylus tip; (3) For accurate measurement of the abraded tip, use a digital binocular, which facilitates the replication of a correct 90° angle, and further reduces the measurement errors; (4) In case of coarse-grained and/or heterogeneous

Table 13 List of published articles, standards and theses on Cerchar test

No.	References	Main contributions
1	Valantin (1973)	Introduction of Cerchar abrasivity test with its index — CAI
2	West (1981)	Discussion on different methods for rock abrasiveness assessment
3	Suana and Peters (1982)	Relation of to mineralogy and petrography of rocks
4	Atkinsion et al. (1986)	Abrasiveness assessment using different parameters (i.e., Schmidt hammer, Schore scleroscope, CAI and toughness index)
5	Cerchar (1986)	Specification for Cerchar abrasivity test (in French)
6	West (1986a)	Correlation of CAI with quartz content; Introduction of West apparatus
7	West (1986b)	Correlation of CAI with Mohs hardness number
8	West (1989)	
9	Atkinson (1993)	Abrasiveness and hardness assessment of hard rocks and their applications
10	Al-Ameen and Waller (1994)	Correlations of CAI with rock strength and abrasive mineral content; Effect of testing distance on CAI; Discussion on Cerchar scratching mechanism
11	NF P94-430-1 (2000)	French standard for Cerchar abrasivity test
12	Mathier and Gisiger (2003)	Relation of CAI to LAC based on basalts taken from Iceland
13	Plinninger et al. (2003)	Discussion on effect of some testing condition-based factors (i.e., testing apparatus; surface rouhness, testing distance) on CAI; Suggestion of 115CrV4 tool steel hardened to HRC 55 as reference; Correlation of CAI with mineralogical parameters (i.e., EQC) of rocks
14	Rostami et al. (2005)	Discussion on effect of surface roughness on CAI; Introduction of a new tip wear measurement approach; Tool lifetime estimation using CAI for TBM discs (CSM model)
15	Michalakopoulos et al. (2006)	Effect of stylus hardness on CAI
16	Fowell and Abu Bakar (2007)	Review on rock abrasiveness measurement methods (i.e., Cerchar and LCPC abrasivity tests)
17	Alber (2008)	Effect of confining pressure on CAI
18	Eberl et al. (2008)	Effect of high temperature on CAI
19	Lassnig et al. (2008)	Effect of mineral grain size on CAI
20	Yarali et al. (2008)	Correlation of CAI with petrographical parameters (e.g., quartz content, quartz grain size and cement degree) of coal sendimentary rocks taken from Turkey; Estimation of drag pick consumption using CAI
21	Jacobs and Hagen (2009)	Effect of some testing condition-based factors (i.e., stylus hardness and metallurgy, applied load, testing distance and duration and rock moisture) on CAI
22	Käsling (2009)	A comprehensive study on Cerchar abrasivity test including testing condition-based factors and rock intrinsic properties (Ph.D. Thesis, TU Munich, Germany)
23	Jacobs and Hagen (2009)	Effect of different testing condition-based factors on CAI
24	Stanford and Hagan (2009)	Effect of stylus hardness and metallurgy on CAI
25	Thuro and Käsling (2009)	Correlation of two abrasivity indexes (Cerchar vs. LCPC) and their classifications
26	Altindag et al. (2010)	Correlation of CAI with rock brittleness index expressed by UCS and BTS in different CAI formulas
27	ASTM D7625-10 (2010)	ASTM norm for Cerchar abrasivity test
28	Ghasemi (2010)	A comprehensive study on effect of testing condition-based factors on CAI. (Master Thesis, Pennsylvania State University, USA)
29	Kahraman et al. (2010)	Prediction of strength properties (i.e., UCS, E) of tectonic rocks by CAI using artifificial neural networks analysis approach
30	Khandelwal and Ranjith (2010)	Relation of P-wave velocity to CAI
31	Deliormanli (2012)	Correlation of CAI with rock strength (i.e., UCS, DSS) and abrasiveness (i.e., BA, WWA) for marble
32	Yarali et al. (2013)	Effect of testing distance on CAI
33	Alber et al. (2014)	ISRM recommendation for Cerchar abrasivity test
34	Hamzaban et al. (2014)	Introduction of a new Cerchar testing device; Application of MCAI for abrasiveness assessment and its relation to CAI
35	Rostami et al. (2014)	Effect of different testing condition-based factors on CAI
36	He et al. (2015)	Introduction of a new Cerchar testing device; Simple and multiple regression analyses of CAI with mechanical and structural properties (i.e., microstructure coefficient) of rocks
37	Kahraman et al. (2015)	Prediction of triaxial strength of tectonic rocks by CAI
38	Majeed and Abu Bakar (2015)	Simple and multiple regression analyses of CAI with mechanical and petrographical parameters of rocks taken from Pakistan

Table 13 (continued)

No.	References	Main contributions
39	Perez et al. (2015)	Feasibility of AE measurements as a manner to predict CAI
40	Tripathy et al. (2015)	Simple and multiple regression analyses of CAI with mechanical and petrographical parameters of rocks taken from India
41	Abu Bakar et al. (2016)	Effect of rock moisture on CAI
42	Er and Tuğrul (2016)	Correlations of CAI with physical and mechanical properties of rocks taken from Turkey. Effect of surface roughness (i.e., roughness, waviness and numbers of peaks) on CAI
43	Ko et al. (2016)	Simple and multiple regression analyses of CAI with mechanical parameters of rocks including cutter life index
44	Moradizadeh et al. (2016)	Correlation of EQC, Is50 with CAI for different types of rock
45	Yarali and Duru (2016)	Effect of testing distance and surface roughness, respectively, on CAI
46	Balani et al. (2017)	DEM modeling of Cerchar rock scratching in consideration of tool wear
47	Cheshomi and Moradhaseli (2017)	Correlation study on different abrasivity parameters (i.e., CAI, LAC, EQC) with each other
48	Ündül and Er (2017)	Simple and multiple regression analyses of CAI with mechanical and mineralogical-petrographical parameters of volcanic rocks
49	Hamzaban et al. (2018)	Application of specific energy (SE_i) for abrasiveness assessment and rock-tool interaction estimation
50	Ozdogan et al. (2018)	Simple and multiple regression analyses of CAI with mechanical parameters of rocks taken from Turkey
51	Piazzetta et al. (2018)	Identification of Cerchar abrasive wear mechanisms on the steel stylus; Relation ofCAI to wear coefficient in tribology
52	Rossi et al. (2018)	Introduction of a new Cerchar testing device; Evaluation of drilling efficiency due to rock heating
53	Torrijo et al. (2018)	Correlation of CAI with chemical compositions and petrography of andesitic rocks taken from Ecuador
54	Aydin (2019)	Effect of some testing condition-based parameters on CAI
55	Kadkhodaei and Ghasemi (2019)	Development of a calculation model for predicting CAI using gene expression programming approach
56	Janc et al. (2020)	Review on different rock abrasiveness assessment methods including Cerchar test
57	Ji et al. (2020)	High temperature effect on CAI based on granite
58	Rossi et al. (2020)	Evaluation of drilling efficiency due to rock heating
59	Teymen (2020)	Simple and multiple regression analyses of CAI with mechanical parameters (i.e., UCS, E, BTS, Is_{50} and K_{IC}) of rocks
60	Zhang (2020)	A special study on rock cutting-related parameters in Cerchar scratch test (Ph.D. Thesis, TU Bergakademie Freiberg, Germany)
61	Zhang and Konietzky (2020)	Application of Cerchar abrasion ratio (CAR) for cutting effectivity evaluation
62	Zhang et al. (2020a)	Application of Cerchar specific energy (CSE) for cutting efficiency evaluation
63	Zhang et al. (2020b)	Study on some in rock cutting meaningful parameters
64	Zhang et al. (2020c)	Effect of testing condition-based factors (i.e., testing distance and velocity, surface roughness, testing distance and velocity and rock anisotropy) on CAI
65	Cheshomi and Moradizadeh (2021)	Correlations of different abrasivity parameters (i.e., CAI, EQC, LAC) with rock strength index calculated from UCS and BTS
66	Gong et al. (2021)	Discussion on CAI classifications and its applications for tool wear estimation (in Chinese)
67	Zhang et al. (2022a)	DEM modeling of Cerchar scratch test in consideration of rock-tool interaction
68	Abu Bakar et al. (2023)	Combined effect of temperature and confining pressure on CAI
69	Hamzaban et al. (2023)	A review on different rock abrasiveness assessment methods
70	Kaspar et al. (2023)	Correlations of CAI with hardness (i.e., Mohs, Rosiwal and Vickers) and UCS of rocks
71	Wang et al. (2023)	Effect of cooling rate after rock heating on CAI
72	Gao et al. (2024)	Database creation for various types of rock based on Cerchar abrasivity test
73	Karrari et al. (2024)	Correlation of CAI with various rock cutting-related parameters
74	Zhang et al. (2024)	High temperature effect on CAI and drilling efficiency

rocks, increase the number of single tests to obtain a more accurate and reliable CAI value; (5) When assessing anisotropic rocks, conduct the tests at least in two different scratching-to-foliation testing directions.

Rock abrasiveness can be related to various mineral- and rock-related factors, including mineral composition and content, grain size, shape and hardness and cement material between grains, as well as intrinsic properties of the

rock (i.e., strength, brittleness and toughness). A single test cannot precisely indicate rock abrasiveness. Instead, a combination of factors provides a more reliable assessment. This highlights the multifaceted nature of abrasiveness, prompting scholars to seek correlations between CAI and various rock physical, mechanical, mineralogical and petrographical parameters. Numerous multivariate linear and non-linear (best-fitting) correlations have been established in this pursuit. Mathematically, increasing the number of variables in a model enhances the correlation coefficient, but it necessitates careful consideration of which factors to include in abrasiveness assessment. Firstly, it is advisable to avoid using complex indexes that rely on fundamental rock properties for correlation studies, because these indexes are derived from basic parameters. Secondly, it is crucial to determine which parameter holds greater significance in influencing the reliability of rock abrasiveness. In a correlation model incorporating multiple parameters, assigning correlation coefficient to each parameter within the equation can illuminate their weight percentage. Thirdly, it is worth noting that correlation models can change with variations in quantity of rock samples for single and multiple regression analyses. Among the rock mechanical properties, compressive, tensile and shear strengths are the most dominant factors, and from the mineralogical aspect, quartz with respect to its size, shape and content, as well as its equivalence, EQC, plays the most important role affecting the abrasiveness. To enhance our understanding of rock abrasiveness, it is anticipated that a more dependable correlation can be established by determining the mode-II fracture toughness of rocks. Additionally, considering a petrographical index like texture coefficient could contribute to assess abrasiveness. The texture coefficient integrates geometric parameters related to both rock matrix and individual mineral grains, including area weighting, perimeter and aspect ratio (defined as the major axis length to minor axis length ratio of the best-fitted ellipse for a given mineral grain). Therefore, a comprehensive parameter that includes mechanical, mineralogical and petrographical properties of rocks may yield more dependable predictions regarding their abrasive potential.

6.2 Perspectives on future research

Analyzing the scratching process in the Cerchar test, it is evident that the stylus penetrates the rock surface, creating a scratch groove characterized by cracks and the extraction of mineral grains. Using the Cerchar testing method is therefore a significant approach for estimating the rock-tool interaction in rock excavation. The newly designed testing device enables the measurements and records of crucial parameters during rock cutting or drilling, especially the scratching force applied and the specific energy consumed for tool movement, the wear volume on the tool surface, the penetration depth within the rock and the material removal from the rock surface. These data serve as valuable indexes for evaluating the cutting or drilling efficiency and excavation effectivity. The Cerchar abrasion ratio (CAR), which considers both the tool wear and material removal, provides a means to estimate rock-tool interaction and to evaluate tool performance. Moreover, this analysis is not limited to soft rocks and can be based on a single test. However, for practical applications, additional field validations are necessary to extend our predictions and correlations regarding rock hardness, strength and abrasiveness beyond laboratory-scaled tests.

In material science and tribology, the Cerchar test is a valuable method for understanding how rock materials respond to the combined forces of indentation and cutting by mechanical tools. To gain insights into the formation of scratch grooves and the removal of rock material during cutting (depending on the depth of cut), both thin-section and SEM analyses are considerable. Additionally, SEM examination of the abraded stylus tip can serve as a valuable reference for detecting the wear phenomenon on mechanical tools. Exploring wear behaviour and tool performance across different tool steels, in consideration of variations in material composition and strength, is a promising avenue for further research.

In rock engineering, particularly in deep geothermal drilling, it is worth noting that drill head wear accelerates, as drilling depth increases. Investigating the effect of high in-situ stresses and temperatures on the rock abrasiveness and tool wear can also be achieved through specialized test setups and experiments.

To advance more understanding of hard rock excavation, the development of a comprehensive Cerchar testing device capable of measuring various parameters related to rock cutting is imperative. This device should include measurements of thrust and cutting forces, cutting distance and velocity, depth of cut and attack angle. Such instrument would prove invaluable for scholars engaged in hard rock excavation projects.

Data availability The data can be available from the authors upon request.

Declarations

Conflict of interest The authors declare that they have no known competing financial interests or personal relationships that could have appeared to influence the work reported in this paper.

References

Abu Bakar MZ, Ali H, Majeed Y (2023) Effects of heat treatment and confining pressure on rock abrasivity and its ramifications for bit wear and drillability in deep geothermal reservoirs. Rock Mech Rock Eng 56:8191–8208. https://doi.org/10.1007/s00603-023-03500-2

Abu Bakar MZ, Majeed Y, Rostami J (2016) Effects of rock water content on Cerchar abrasivity index. Wear 368–369:132–145. https://doi.org/10.1016/j.wear.2016.09.007

Al-Ameen SI, Waller MD (1994) The influence of rock strength and abrasive mineral content on the Cerchar abrasive index. Eng Geol 36:293–301. https://doi.org/10.1016/0013-7952(94)90010-8

Alber M, Yarali O, Dahl F, Bruland A, Käsling H, Michalakopoulos TN, Cardu M, Hagan P, Aydin H, Özarslan A (2014) ISRM suggested method for determining the abrasivity of rock by the Cerchar abrasivity test. Rock Mech Rock Eng 47:261–266. https://doi.org/10.1007/s00603-013-0518-0

Alber M (2008) Stress dependency of the Cerchar abrasivity index (CAI) and its effects on wear of selected rock cutting tools. Tunn Undergr Sp Technol 23:351–359. https://doi.org/10.1016/j.tust.2007.05.008

Altindag R, Sengun N, Sarac S, Mutluturk M, Guney A (2010) Evaluating the relations between brittleness and Cerchar abrasion index of rocks. In: Rock Engineering in Difficult Ground Conditions—Soft rocks and Karst

ASTM D7625-10 (2010) Standard test method for laboratory determination of abrasiveness of rock using the Cerchar method. ASTM International

Atkinson T, Cassapi VB, Singh I (1986) Assessment of abrasive wear resistance potential in rock excavation machinery. Int J Min Geol Eng 3:151–163. https://doi.org/10.1007/BF01560672

Atkinson RH (1993) Hardness tests for rock characterization. Rock testing and site characterization. Pergamon, Oxford, pp 105–117

Aydin H (2019) Investigating the effects of various testing parameters on Cerchar abrasivity indx and its repeatability. Wear 418–419:61–74. https://doi.org/10.1016/j.wear.2018.11.001

Balani A, Chakeri H, Barzegari G, Ozcelik Y (2017) Investigation of various parameters effect on Cerchar abrasivity index with PFC3D modeling. Geotech Geol Eng. https://doi.org/10.1007/s10706-017-0275-z

Bieniawski ZT, Celada CB, Galera JM, Tardaguila IG (2009) Prediction of cutter wear using RME. In: ITA-ITAES world tunnel Congress, Budapest, Hungary

Bilgin N (1989) Applied rock excavation for civil and mining eng. Istanbul, Birsen Yayinevi, p 192

Bołoz Ł, Biały W (2023) Methods and test benches for cutting tools testing—A review. Energies 16:445. https://doi.org/10.3390/en16010445

Bruland A (1998) Drillability test methods. NTNU Trondheim

Büchi E (1984) Einfluss Geologischer Parameter auf die Vortriebsleistung einer Tunnelbohrmaschine. Ph.D. Thesis, Universität Bern (**in German**)

Büchi E, Mathier JF, Wyss C (1995) Gesteinsabrasivität—ein bedeutender Kostenfaktor beim mechanischen Abbau von Fest- und Lockergesteinen. Tunnel 5:38–43 (**in German**)

Burwell JT (1957) Survey of possible wear mechanisms. Wear 1:119–141

Capik M, Yilmaz AO (2017) Modeling of micro deval abrasion loss based on some rock properties. J Afr Earth Sci 134:549–556. https://doi.org/10.1016/j.jafrearsci.2017.04.006

Capik M, Yilmaz AO (2021) Development models for the drill bit lifetime prediction and bit wear types. Int J Rock Mech Min Sci 139:104633. https://doi.org/10.1016/j.ijrmms.2021.104633

Cassapi VB (1987) Application of rock hardness and abrasive indexing to rock excavating equipment selection. University of Nottingham

Cerchar (1986) Centre d'Etudes et des Recherches des Charbonages de France, Verneuil (**in French**)

Cheshomi A, Moradhaseli S (2017) Effect of petrographic characteristics on abrasive properties of granitic building stones. Q J Eng Geol Hydrogeol. https://doi.org/10.1144/qjegh2016-048

Cheshomi A, Moradizadeh M (2021) The relationship between strength and abrasion characterizations in granite building stones. Q J Eng Geol Hydrogeol. https://doi.org/10.1144/qjegh2020-045

Chong KP, Kuruppu MD (1984) New specimen for fracture toughness determination for rock and other materials. Int J Fract 26:59–62. https://doi.org/10.1007/BF01157555

Comakli R (2019) Effects of the physico-mechanical properties of low-strength pyroclastic rocks on cutter wear of roadheaders. Wear 428–429:205–216. https://doi.org/10.1016/j.wear.2019.03.014

Dahl F, Bruland A, Jakobsen PD, Nilsen B, Grøv E (2012) Classifications of properties influencing the drillability of rocks, based on the NTNU/SINTEF test method. Tunn Undergr Sp Technol 28:150–158. https://doi.org/10.1016/j.tust.2011.10.006

Deketh HJR (1995) Wear of rock cutting tools laboratory experiments on the abrasivity of rock. A.A. Balkema, Rotterdam, p 143

Deliormanli AH (2012) Cerchar abrasivity index (CAI) and its relation to strength and abrasion test methods for marble stones. Constr Build Mater 30:16–21. https://doi.org/10.1016/j.conbuildmat.2011.11.023

Eberl S, Restner U, Galler R, Mali H (2008) The influence of the parameter "temperature" on the abrasiveness of rock. Geomech Tunn. https://doi.org/10.1002/geot.200800009

Ellecosta P, Kasling H, Thuro K (2018) Tool wear in TBM hard rock drilling—backgrounds and special phenomena. Geomech Tunn 11:2. https://doi.org/10.1002/geot.201800006

EN 14157 (2017) Natural stone test methods—Determination of the abrasion resistance. CEN Committee, Brussels

Er S, Tuğrul A (2016) Correlation of physico-mechanical properties of granitic rocks with Cerchar abrasivity index in Turkey. Measurement 91:114–123. https://doi.org/10.1016/j.measurement.2016.05.034

Janc B, Jovicic V, Vukelic Z (2020) Laboratory test methods for assessing the abrasivity of rocks and soils in geotechnology and mining applications. Mater Geoenviron 67:103−118. https://doi.org/10.2478/rmzmag-2020-0012

Evans I (1958) Theoretical aspect of coal ploughing. Mechanical properties of non-metallic brittle materials. Butterworths, London, pp 451–468

Farrokh E, Kim DY (2018) A discussion on hard rock TBM cutter wear and cutterhead intervention interval length evaluation. Tunn Undergr Sp Technol 81:336–357. https://doi.org/10.1016/j.tust.2018.07.017

Figarska-Warchoł B, Rembiś M (2021) Lamination and its impact on the physical and mechanical properties of the Permian and Triassic terrestrial sandstones. Resources 10:42. https://doi.org/10.3390/resources10050042

Fowell RJ, Abu Bakar MZ (2007) A review of the Cerchar and LCPC rock abrasivity measurement methond. In: 11th Congress of the international society for rock mechanics, p 6

Frenzel C, Käsling H, Thuro K (2008) Factors influencing disc cutter wear. Geomech Tunn 1:55–60. https://doi.org/10.1002/geot.200800006

Frenzel C (2011) Disc cutter wear phenomenology and their implications on disc cutter consumption for TBM. ARMA, pp 11−211

Gehring K (1995) Leistungs- und Verschleißprognosen im maschinellen. Tunn Felsbau 13:439–448 (**in German**)

Ghasemi A (2010) Study of Cerchar abrasivity index and potential modifications for more consistent measurement of rock abrasion. Master Thesis, Pennsylvania State University

Gong QM, Xu HY, Li LM (2021) Discussions on the rock abrasivity index classification. Chin J Undergr Sp Eng 17(3):748–758 (**in Chinese**)

Hamzaban MT, Memarian H, Rostami J (2018) Determination of scratching energy index for Cerchar abrasion test. J Min Environ 9:73–89. https://doi.org/10.22044/jme.2017.5738.1389

Hamzaban MT, Memarian H, Rostami J, Ghasemi-Monfared H (2014) Study of rock-pin interaction in cerchar abrasivity test. Int J Rock Mech Min Sci 72:100–108. https://doi.org/10.1016/j.ijrmms.2014.09.007

Hamzaban MT, Rostami J, Dahl F, Macias FJ, Jakobsen PD (2023) Wear of cutting tools in hard rock excavation process: a critical review of rock abrasiveness testing methods. Rock Mech Rock Eng 56:1843–1882. https://doi.org/10.1007/s00603-022-03187-x

He JM, Li SD, Li X, Wang X, Guo JY (2015) Study on the correlations between abrasiveness and mechanical properties of rocks combining with the microstructure characteristic. Rock Mech Rock Eng. https://doi.org/10.1007/s00603-015-0862-3

Howarth DF, Rowlands JC (1987) Quantitative assessment of rock texture and correlation with drillability and strength properties. Int J Rock Mech Min Sci Geomech Abstr 24:57–85. https://doi.org/10.1016/0148-9062(87)90997-1

Huang HY, Detournay E (2012) Discrete element modeling of tool-rock interaction II: rock indentation. Int J Numer Anal Methods Geomech. https://doi.org/10.1002/nag.2114

Huang HY, Lecampion B, Detournay E (2013) Discrete element modeling of tool-rock interaction I: rock cutting. Int J Numer Anal Methods Geomech 37:1913–1329. https://doi.org/10.1002/nag.2113

Hucka V, Das B (1974) Brittleness determination of rocks by different methods. Int J Rock Mech Min Sci Geomech Abstr 11:389–392. https://doi.org/10.1016/0148-9062(74)91109-7

Irwin GR (1958) Fracture, elasticity and plasticity. Springer, Berlin, pp 551–590

ISRM (1988) Suggested methods for determining the fracture toughness of rock. Int J Rock Mech Min Sci Geomech Abstr 25:71–96

Itasca (1999) Itasca Consulting Group Inc. PFC (Particle Flow Code), Version 3.0

Itasca (2014) Itasca Consulting Group Inc. PFC (Particle Flow Code), Version 5.0

Jacobs N, Hagen P (2009) The effect of stylus hardness and some test parameters on Cerchar abrasivity index. In: 43rd US rock mechanics symposium and 4th U.S.-Canada rock mechanics symposium. ARMA, pp 09–191

Ji Y, Wang L, Zheng Y, Wu W (2020) Temperature-dependent abrasivity of Bukit Timah granite and implications for drill bit wear in thermo-mechanical drilling. Acta Geotech. https://doi.org/10.1007/s11440-020-01056-x

Johnson ST, Fowell RJ (1986) Compressive strength is not enough (Assessing pick wear for drag tool-equiped machines). In: 27th US symposium rock mechanics, Tuscaloosa, USA, pp 840–845

Kadkhodaei MH, Ghasemi E (2019) Development of a GEP model to assess Cerchar abrasivity index of rocks based on geomechanical properties. J Min Environ 10:917–928. https://doi.org/10.22044/jme.2019.8141.1684

Kahraman S, Alber M, Fener M, Gunaydin O (2010) The usability of Cerchar abrasivity index for the prediction of UCS and E of Misis Fault Breccia: regression and artificial neural networks analysis. Expert Syst Appl 37:8750–8756. https://doi.org/10.1016/j.eswa.2010.06.039

Kahraman S, Alber M, Gunaydin O, Fener M (2015) The usability of the Cerchar abrasivity index for the evaluation of the triaxial strength of Misis Fault Breccia. Bull Eng Geol Env 74:163–170. https://doi.org/10.1007/s10064-014-0618-4

Karrari SS, Heidari M, Hamidi JK, Teshnizi ES (2024) New Cerchar device used for evaluating Cerchar abrasivity parameters. Int J Geomech 24(3):04024005. https://doi.org/10.1061/IJGNAI.GMENG-8676

Käsling H (2009) Bestimmung der Gesteinsabrasivität—Grundlagen, Anwendung und Einsatzgrenzen bei maschinellen Tunnelvortrieben. Ph.D. Thesis, TU München (**in German**)

Käsling H, Thiele I, Thuro K (2007) Abrasivity investigations with the Cerchar scratch test—an evaluation of the testing conditions. In: Tagung für Ingenieurgeologie und Forum "Junge Ingenieurgeologen", Bochum, pp 229–235

Käsling H, Thuro K (2010) Bestimmung der Gesteinsabrasivität—Versuchstechniken und Anwendung. In: Baugrundtagung. Deutsche Gesellschaft für Geotechnik e.V., München, pp 233–240 (**in German**)

Kaspar M, Latal C, Pittino G, Blümel M (2023) Hardness, strength and abrasivity of rocks: correlations and predictions. Geomech Tunn 16(2):184–192. https://doi.org/10.1002/geot.202200007

Khandelwal M, Ranjith PG (2010) Correlating index properties of rocks with P-wave measurements. J Appl Geophys 71:1–5. https://doi.org/10.1016/j.jappgeo.2010.01.007

Ko TY, Kim TK, Son Y, Jeon S (2016) Effect of geomechanical properties on Cerchar Abrasivity Index (CAI) and its application to TBM tunnelling. Tunn Undergr Sp Technol 57:99–111. https://doi.org/10.1016/j.tust.2016.02.006

Küpferle J, Röttger A, Theisen W, Alber M (2015) Abrasivity of rock and soil

Lassnig K, Latal C, Klima K (2008) Impact of grain size on the Cerchar abrasiveness test. Geomech Tunn 1:71–76. https://doi.org/10.1002/geot.200800008

Liu QS, Liu JP, Pan YC, Zhang XP, Peng XX, Gong QM, Du LJ (2017) A wear rule and cutter life prediction model of a 20 inch TBM cutter for Granite: a case study of a water conveyance tunnel in China. Rock Mech Rock Eng 50:1303–1320

Macias FJ, Dahl F, Bruland A (2015) New rock abrasivity test method for tool life assessments on hard rock tunnel boring: the rolling indentation abrasion test (RIAT). Rock Mech Rock Eng. https://doi.org/10.1007/s00603-015-0854-3

Maidl B, Schmid L, Ritz W, Herrenknecht M (2001) Tunnelbohrmaschinen im Hartgestein. Ernst & Sohn Verlag, Berlin (**in German**)

Majeed Y, Abu Bakar MZ (2015) Statistical evaluation of Cerchar abrasivity index (CAI) measurement methods and dependence on petrographic and mechanical properties of selected rocks of Pakistan. Bull Eng Geol Environ. https://doi.org/10.1007/s10064-015-0799-5

Majeed Y, Abu Bakar MZ, Butt IA (2019) Abrasivity evaluation for wear prediction of button drill bits using geotechnical rock properties. Bull Eng Geol Environ. https://doi.org/10.1007/s10064-019-01587-y

Matern NV, Hjelmer A (1943) Tests with chippings, Stockholm

Mathier JF, Gisiger JP (2003) Abrasivity of Icelandic basalts. In: ISRM 2003—Technology roadmap for rock mechanics, South African Institute of Mining and Metallurgy, p 3

McFeat-Smith I, Fowell RJ (1977) Correlation of rock properties and the cutting performance of tunnelling machines. Int J Rock Mech

Min Sci Geomech Abstr. https://doi.org/10.1016/0148-9062(77)90837-3
Michalakopoulos TN, Anagnostou VG, Bassanou ME, Panagiotou GN (2006) The influence of steel styli hardness on the Cerchar abrasiveness index value. Int J Rock Mech Min Sci 43:321–327. https://doi.org/10.1016/j.ijrmms.2005.06.009
Moore MA (1974) A review of two-body abrasive wear. Wear 27:1–17
Moore MA, King FS (1980) Abrasive wear of brittle solids. Wear 60:123–140
Moradizadeh M, Cheshomi A, Ghafoori M, TrighAzali S (2016) Correlation of equivalent quartz content, slake durability index and Is_{50} with Cerchar abrasiveness index for different types of rock. Int J Rock Mech Min Sci 86:42–47. https://doi.org/10.1016/j.ijrmms.2016.04.003
Mucha K (2023) Application of rock abrasiveness and rock abrasivity test methods—A review. Sustainability 15:11243. https://doi.org/10.3390/su151411243
Münch D, Bortoleto EM, Lima RMF (2023) Analysis of the effect of a banded structure on jaspilite abrasiveness. Wear 530–531:204960. https://doi.org/10.1016/j.wear.2023.204960
NF P18-579 (1990) Granulats—Essai d'abrasivite et de broyabilite, Paris (**in French**)
NF P94-430-1 (2000) Roches—Determination du pouvoir abrasif d'une roche—Partie 1: essai de rayure avec une pointe, Paris (**in French**)
Nishimatsu Y (1972) The mechanics of rock cutting. Int J Rock Mech Min Sci Geomech Abstr 9:261–270. https://doi.org/10.1016/0148-9062(72)90027-7
Nizamoglu S (1978) Contrubution a L'etude du Fonctionnement des Tunneliers "Plein Section" et Analysc de L'usure de Leurs Outils de Coupe. These Pour Obtenir le Grade de Docteur Ing. Ecole des Mines de Nancy, p 139 (**in French**)
Okubo S, Fukui K, Nishimatsu Y (2011) Estimating abrasivity of rock by laboratory and in situ tests. Rock Mech Rock Eng 44:231–244. https://doi.org/10.1007/s00603-010-0113-6
Ozdogan MV, Deliormanli AH, Yenice H (2018) The correlations between the Cerchar abrasivity index and the geomechanical properties of building stones. Arab J Geosci. https://doi.org/10.1007/s12517-018-3958-8
Perez S, Karakus M, Sepulveda E (2015) A preliminary study on the role of acoustic emission on inferring Cerchar abrasivity index of rocks using artifical neural network. Wear 344–345:1–8. https://doi.org/10.1016/j.wear.2015.10.006
Piazzetta GR, Lagoeiro LE, Figueira IFR, Rabelo MAG, Pintaude G (2018) Identification of abrasion regimes based on mechanisms of wear on the steel stylus used in the Cerchar abrasiveness test. Wear 410–411:181–189. https://doi.org/10.1016/j.wear.2018.07.009
Plinninger RJ (2002) Klassifizierung und Prognose von Werkzeugverschleiß bei konventionellen Gebirgslösungsverfahren im Festgestein. Münchner Geologische Heft Reihe B, Angewandte Geologie, 17, München (**in German**)
Plinninger RJ (2015) Abrasivitätsprüfung—quo vadis? Hintergründe, Stand der Normung und Fallbeispiele zur Bewertung der Abrasivität von Fest- und Lockergesteinen. In: Symposium für Aufbereitungstechnik, Freiberg (**in German**)
Plinninger RJ, Käsling H, Thuro K (2004) Wear prediction in hardrock excavation using the Cerchar abrasiveness index (CAI). In: EUROCK 2004 and 53nd geomechanics colloquium. VGE
Plinninger RJ, Käsling H, Thuro K, Spaun G (2003) Testing conditions and geomechanical properties influencing the Cerchar abrasiveness index (CAI) value. Int J Rock Mech Min Sci 40:259–263. https://doi.org/10.1016/S1365-1609(02)00140-5
Restner U, Pichler J (2007) Mont cenis tunnel modification project—lowering of tunnel invert with sandvik tunnel miner MT620. In 2nd Symposium on underground excavations for transportation, 15–17 Nov 2007, Istanbul, Turkey.
Rojek J, Onate E, Labra C, Kargl H (2011) Discrete element simulation of rock cutting. Int J Rock Mech Min Sci 48:993–1010. https://doi.org/10.1016/j.ijrmms.2011.06.003
Rosiwal, A. (1916). Neuere Ergebnisse der Härtebestimmung von Mineralien und Gesteinen. Ein absolutes Maß für die Härtespröder Körper. Verhandlg d kk geol R-A:117−147, Wien
Rossi E, Kant MA, Borkeloh O, Saar MO, Rudolf von Rohr P (2018) Experiments on rock-bit interaction during a combined thermo-mechanical drilling method. In: 43rd workshop on Geothermal Reservoir Engineering, Stanford
Rossi E, Saar MO, Von Rohr PR (2020) The influence of thermal treatment on rock-bit interaction: a study of a combined thermo-mechanical drilling (CTMD) concept. Geotherm Energy 8:16. https://doi.org/10.1186/s40517-020-00171-y
Rostami J, Ghasemi A, Gharahbagh EA, Dogruoz C, Dahl F (2014) Study of dominant factors affecting Cerchar abrasivity index. Rock Mech Rock Eng 47:1905–1919. https://doi.org/10.1007/s00603-013-0487-3
Rostami J, Ozdemir L, Bruland A, Dahl F (2005) Review of issues related to cerchar abrasivity testing and their implications on geotechnical investigations and cutter cost estimates. In: Rapid excavation and tunneling conference (RETC), Seattle, USA, pp 738−751
Schimazek J, Knatz H (1970) The influence of rock composition on cutting velocity and chisel wear of tunnelling machines. Glückauf 106:274–278 (**in German**)
Schimazek J, Knatz H (1976) The assessment of cuttability of rocks by drag and roller bits. Erzmetall 29:113–119
Schumacher L (2004) Auslegung und Einsatzbedingung von Tunnelvortriebsmaschinen im Hartgestein. Felsbau 22:21–28 (**in German**)
Selmer-Olsen R, Lien R (1960) Bergartens borbarhet og sprengbarhet (**in Norwegian**)
Gao KD, Wang XY, Wei HX, Wang SX, Xu WP, Li X, Sun LQ, Jiang HX (2024) Abrasivity database of different genetic rocks based on Cerchar abrasivity Test. Scientific Data, 11:630. https://doi.org/10.1038/s41597-024-03470-2
Sievers H (1950) Die bestimmung des bohrwiderstands von gesteinen. Glückauf 37–38:776–784 (**in German**)
Sotoudeh F, Memarian H, Hamzaban MT, Rostami J (2014) Improvement of testing accuracy by a new generation of Cerchar abrasivity testing device. In: North American tunneling conference, Los Angeles, CA, pp 211−217
Stanford J, Hagan P (2009) An assessment of the impact of stylus metallurgy on Cerchar abrasiveness index. In: Coal operators' conference, pp 348–355
Su O, Akcin NA (2011) Numerical simulation of rock cutting using the discrete element method. Int J Rock Mech Min Sci 48:434–442. https://doi.org/10.1016/j.ijrmms.2010.08.012
Suana M, Peters T (1982) Cerchar abrasivity index and its relation to rock mineralogy and petrography. Rock Mech 15:1–8. https://doi.org/10.1016/0148-9062(82)91413-9
Teymen A (2020) The usability of Cerchar abrasivity index for the estimation of mechanical rock properties. Int J Rock Mech Min Sci 128:104258. https://doi.org/10.1016/j.ijrmms.2020.104258
Thuro K (1996) Bohrbarkeit beim konventionellen Sprengvortrieb. Münchner geologische Hefte Reihe B, Angewandte Geologie (**in German**)
Thuro K (2002) Geologisch-felsmechanische Grundlagen der Gebirgslösung im Tunnelbau. Münchner geologische Hefte Reihe B, Angewandte Geologie (**in German**)
Thuro K, Käsling H (2009) Classification of the abrasiveness of soil and rock. Geomech Tunn 2:179–188. https://doi.org/10.1002/geot.200900012

Torrijo FJ, Garzon-Roca J, Company J, Cobos G (2018) Estimation of Cerchar abrasivity index of andesitic rocks in Ecuador from chemical compounds and petrographical properties using regression analyses. Bull Eng Geol Environ. https://doi.org/10.1007/s10064-018-1306-6

Tripathy A, Singh TN, Kundu J (2015) Prediction of abrasiveness index of some Indian rocks using soft computing methods. Measurement 68:302–309. https://doi.org/10.1016/j.measurement.2015.03.009

Ündül Ö, Er S (2017) Investigating the effects of micro-texture and geo-mechanical properties on the abrasiveness of volcanic rocks. Eng Geol 229:85–94. https://doi.org/10.1016/j.enggeo.2017.09.022

Valantin A (1973) Test Cerchar por la mesure de la dureté et de l'abrasivité des roches. Annexe de l'exposée présent aux Journées de Information "Techniques de creusement" (**in French**)

Van Wyk G, Els DNJ, Akdogan G, Bradshaw SM, Sacks N (2014) Discrete element simulation of tribological interactions in rock cutting. Int J Rock Mech Min Sci 65:8–19. https://doi.org/10.1016/j.ijrmms.2013.10.003

Verhoef PNW (1997) Wear of rock cutting tools—Implications for the site investigation of rock dredging projects. A.A. Balkema, Rotterdam

Wang CY, Clausen R (2002) Marble cutting with single point cutting tool and diamond segments. Int J Mach Tools Manuf 42:1045–1054

Wang L, Guo K, Wu W (2023) Abrasivity measurement of brittle rock after thermal treatment. Measurement 212(15):112710. https://doi.org/10.1016/j.measurement.2023.112710

West G (1981) A review of rock abrasiveness testing for tunnelling. In: International symposium on weak rock, 21–24 Sept 1981, Tokyo, Japan, pp 585–594

West G (1986a) A relation between abrasiveness and quartz content for some coal measures sediments. Int J Min Geol Eng 4:73–78

West G (1986b) An observation on Mohs' scale of hardness. Q J Eng Geol 19(2):203–205

West G (1989) Rock abrasiveness testing for tunnelling. Int J Rock Mech Min Sci Geomech Abstr 26:151–160. https://doi.org/10.1016/0148-9062(89)90003-X

Wijk G (1992) A model of tunnel boring machine performance. Geotech Geol Eng 10:19–40

Wilfing LSF (2016) The Influence of geotechnical parameters on penetration prediction in TBM tunneling in hard rock—Special focus on the parameter of rock toughness and discontinuity pattern in rock mass. Ph.D. Thesis, TU München

Yagiz S (2009) Assessment of brittleness using rock strength and density with punch penetration test. Tunn Undergr Sp Technol 24:66–74

Yarali O, Aydin H, Duru H, Özarslan A (2013) Effect of scratch length on the Cerchar abrasivity index. Rock mechanics for resources, energy and environment. Tylor and Francis Group, London, pp 369–375

Yarali O, Duru H (2016) Investigation into effect of scratch length and surface condition on Cerchar abrasivity index. Tunn Undergr Sp Technol 60:111–120. https://doi.org/10.1016/j.tust.2016.08.005

Yarali O, Yaşar E, Bacak G, Ranjith PG (2008) A study of rock abrasivity and tool wear in Coal Measures Rocks. Int J Coal Geol 74:53–66. https://doi.org/10.1016/j.coal.2007.09.007

Yasar S, Capik M, Yilmaz AO (2015) Cuttability assessment using the drilling rate index (DRI). Bull Eng Geol Environ. https://doi.org/10.1007/s10064-014-0715-4

Zhang GZ (2020) Cerchar abrasivity test: Laboratory tests and numerical simulation. Ph.D. Thesis, TU Bergakademie Freiberg, p 185

Zhang GZ, Konietzky H (2020) Cerchar abrasion ratio (CAR) as a new indicator for assessing rock abrasivity, rock-stylus interaction and cutting efficiency. Rock Mech Rock Eng. https://doi.org/10.1007/s00603-020-02112-4

Zhang GZ, Konietzky H, Frühwirt T (2020a) Investigation of scratching specific energy in the Cerchar abrasivity test and its application for evaluating rock-tool interaction and efficiency of rock cutting. Wear 448–449:203218. https://doi.org/10.1016/j.wear.2020.203218

Zhang GZ, Konietzky H, Frühwirt T (2024) Experimental investigation of abrasive potential and drilling efficiency at elevated temperatures via Cerchar rock scratching. Geomech Geophys Geo Energy Geo Resour. https://doi.org/10.1007/s40948-024-00831-4

Zhang GZ, Konietzky H, Song ZY, Zhang M (2020b) Study of Cerchar abrasive parameters and their relations to intrinsic properties of rocks for construction. Constr Build Mater 244:118327. https://doi.org/10.1016/j.conbuildmat.2020.118327

Zhang GZ, Konietzky H, Song ZY, Huang S (2020c) Study of some testing condition-based factors affecting the Cerchar abrasivity index (CAI) Arabian. J Geosci 13:1254. https://doi.org/10.1007/s12517-020-06254-1

Zhang GZ, Dang WG, Herbst M, Song ZY (2020d) Complex analysis of rock cutting with consideration of rock-tool interaction using distinct element method (DEM). Geomech Eng 20(5):421–432. https://doi.org/10.12989/gae.2020.20.5.421

Zhang GZ, Bai QS, Herbst M, Zhao J (2022a) Experimental and numerical investigations of Cerchar scratching rock interaction. Int J Geomech 22(4):04022017–04022021. https://doi.org/10.1061/(ASCE)GM.1943-5622.0002317

Zhang GZ, Thuro K, Konietzky H, Menschik FM, Käsling H, Bayerl M (2022b) In-situ investigation of drilling performance and bit wear on an electrical drill hammer. Tunn Undergr Sp Technol 122:104348. https://doi.org/10.1016/j.tust.2021.104348

Zhang ZQ, Zhang KJ, Dong WJ (2021) Experimental investigation on the influence factors on TBM cutter wear based on composite abrasion test. Rock Mech Rock Eng 54:6533–6547. https://doi.org/10.1007/s00603-021-02621-w

Zum Gahr KH (1987) Microstructure and wear of materials, vol 10. Tribology series. Elsevier, Amsterdam